Zentrum für Entwicklungsforschung
Center for Development Research
University of Bonn

ZEF-Discussion Papers on
Development Policy No. 193

Quang Bao Le, Ephraim Nkonya and Alisher Mirzabaev

Biomass Productivity-Based Mapping of Global Land Degradation Hotspots

Bonn, July 2014

The **CENTER FOR DEVELOPMENT RESEARCH (ZEF)** was established in 1995 as an international, interdisciplinary research institute at the University of Bonn. Research and teaching at ZEF addresses political, economic and ecological development problems. ZEF closely cooperates with national and international partners in research and development organizations. For information, see: www.zef.de.

ZEF – Discussion Papers on Development Policy are intended to stimulate discussion among researchers, practitioners and policy makers on current and emerging development issues. Each paper has been exposed to an internal discussion within the Center for Development Research (ZEF) and an external review. The papers mostly reflect work in progress. The Editorial Committee of the ZEF – DISCUSSION PAPERS ON DEVELOPMENT POLICY include Joachim von Braun (Chair), Solvey Gerke, and Manfred Denich. Tobias Wünscher is Managing Editor of the series.

Quang Bao Le, Ephraim Nkonya and Alisher Mirzabaev, Biomass Productivity-Based Mapping of Global Land Degradation Hotspots, ZEF - Discussion Papers on Development Policy No. 193, Center for Development Research, Bonn, July 2014, pp.57.

ISSN: 1436-9931

Published by:
Zentrum für Entwicklungsforschung (ZEF)
Center for Development Research
Walter-Flex-Straße 3
D – 53113 Bonn
Germany
Phone: +49-228-73-1861
Fax: +49-228-73-1869
E-Mail: zef@uni-bonn.de
www.zef.de

The authors:
Quang Bao Le, Swiss Federal Institute of Technology (ETH) Zurich. Contact: quang.le@env.ethz.ch
Ephraim Nkonya, The International Food Policy Research Institute (IFPRI). Contact: e.nkonya@cgiar.org
Alisher Mirzabaev, Center for Development Research (ZEF), University of Bonn. Contact: almir@uni- bonn.de

With the financial support
of the Federal Ministry for Economic Cooperation and Development, Germany

This publication is a scientific contribution to the Economics of Land Degradation Initiative

http://www.eld-initiative.org

Acknowledgements

We would like to thank numerous institutions, colleagues and friends for their support on this paper. We would like, first of all, to thank the German Federal Ministry for Economic Cooperation and Development (BMZ) for financial support to conduct this research. We greatly thank the Review Panel, consisting of Professor Rattan Lal, Dr. Zhanguo Bai and Dr. Paul Reich for their critical and highly useful comments and suggestions. We are highly grateful for colleagues at ZEF and IFPRI, especially Joachim von Braun, Kato Edward, Hoyoung Kwon, Weston Anderson, Alessandro de Pinto and Valerie Graw for their suggestions on the earlier versions of this paper. We also greatly appreciate the comments received from the participants of the ZEF-IFPRI session on “How to mobilize societal change to address land degradation and reduce poverty in the developing world: the role of local policy actions?" organized during the Global Soils Week on 30th October 2013 in Berlin, Germany. Last but not least, we would like to thank Jann Goedecke and Weston Anderson for their outstanding research support in preparing this publication.

Quang Bao Le, Alisher Mirzabaev and Ephraim Nkonya

Abstract

Land degradation is a global problem affecting negatively the livelihoods and food security of billions of people, especially farmers and pastoralists in the developing countries. Eradicating extreme poverty without adequately addressing land degradation is highly unlikely. Given the importance and magnitude of the problem, there have been recurring efforts by the international community to identify the extent and severity of land degradation in global scale. As discussed in this paper, many previous studies were challenged by lack of appropriate data or shortcomings of their methodological approaches. In this paper, using global level remotely sensed vegetation index data, we identify the hotspots of land degradation in the world across major land cover types. In doing so, we use the long-term trend of inter-annual vegetation index as an indicator of biomass production decline or improvement. Besides the elimination of technical factors, confounding the relationship between the indicator and the biomass production of the land, we apply a methodology which accounts for masking effects of both inter-annual rainfall variation and atmospheric fertilization. We also delineate the areas where chemical fertilization could be hiding the inherent land degradation processes.

Our findings show that land degradation hotpots cover about 29% of global land area and are happening in all agro-ecologies and land cover types. Land degradation is especially massive in grasslands. About 3.2 billion people reside in these degrading areas. However, the number of people affected by land degradation is likely to be higher as more people depend on the continuous flow of ecosystem goods and services from these affected areas. As we note in the paper, this figure, although, does not include all possible areas with degraded lands, it identifies those areas where land degradation is most acute and requires priority actions in both in-depth research and management measures to combat land degradation. Our findings indicate that, in fact, land improvement has also occurred in about 2.7% of global land area during the last three decades, providing a support that with appropriate actions land degradation trend could be reversed, and that the efforts to address land degradation need to be substantially increased, at least by a factor, to attain the vision of Zero Net Land Degradation. We also identify concrete aspects in which these results should be interpreted with caution, the limitations of this work and the key areas for future research.

Keywords: land degradation hotspots, mapping, carbon fertilization, Economics of Land Degradation

JEL classification: Q01, Q15, Q23, Q24, Q56

Table of Contents

List of Tables

List of Figures

List of Abbreviations

AVHRR	Advanced Very High Resolution Radiometer
BMZ	German Federal Ministry for Economic Cooperation and Development
ELD	Economics of Land Degradation
EU	European Union
FAO	United Nation's Food and Agriculture Organization
GADM	Database of Global Administrative Areas
GDP	Gross domestic product
GIMMS	Global Inventory Modeling and Mapping Studies
GIS	Geographic Information System
ISRIC	International Soil Reference and Information Center
IFPRI	International Center for Food Policy Research
NDVI	Normalized Differenced Vegetation Index
NGO	Non-Governmental Organization
NOAA	U.S. National Oceanic and Atmospheric Association
NPP	Net Primary Production
PES	Payment for Ecosystem Services
SSA	Sub-Saharan Africa
SLM	Sustainable Land Management
UNCCD	United Nations Convention to Combat Desertification
UNEP	United Nations Environment Program
USD	United States Dollars
USDA-NRCS	United States Department of Agriculture, Natural Resources Conservation
SRTM	Shuttle Radar Topography Mission
TEV	Total Economic Value
ZEF	Center for Development Research, University of Bonn

1. Introduction

Land degradation is a global problem affecting at least a quarter of the global land area (Lal *et al.*, 2012) and seriously undermining the livelihoods, especially of the poor, in all agro-ecologies across the world (Nkonya *et al.*, 2011). Although land degradation has been critical problem throughout the history (Diamond, 2005), it has attained its current global scales, becoming a major global issue especially since the second half of the 20th century (Nkonya *et al.*, 2011). Since the first global mapping of desertification in 1977 (Dregne, 1977), there have been numerous efforts at global mapping of land degradation (Oldeman *et al.*, 1990; USDA-NRCS, 1998; Eswaran *et al.*, 2001). The earlier generation of these studies had been constrained by lack of global level quantitative data which could be used for mapping soil and land degradation, and therefore were based on expert opinions. The developments in the remote sensing and satellite technologies allowed the later studies to be based on quantitative satellite data, such as Global Inventory Modelling and Mapping Studies (GIMMS) dataset of 64 km^2-resolution of Normalized Difference Vegetation Index (NDVI) data, however, several methodological challenges still exist on more accurately estimating the land degradation hotspots (Vlek *et al.*, 2010; Le *et al.*, 2012).

In this context, addressing land degradation may require channeling substantial amounts of scarce resources and making long-term investments. These investments are likely to yield high levels of social returns and welfare improvements. However, all countries in the world have budgetary constraints, necessitating the prioritization of such investments. To combat land degradation, both on the international and national levels, policy makers often need information about areas of severe degradation in order to prioritize national budgets and plan strategic interventions (Vlek *et al.*, 2010; Vogt *et al.*, 2011; Le *et al.*, 2012). To achieve this, accurate maps of land degradation hotspots – where land degradation is most acute, are needed. This study seeks to meet that objective at the global level.

As indicated above, there have been several efforts in the past to map land degradation at the global scale. The major objective of this global study is the identification of regions *where* degradation magnitude and extent are ***relatively high***, i.e., ***geographic degradation hotspots***, for ***prioritizing*** both preventive investments for the restoration or reclamation of degraded land, and subsequent focal ground-based studies. Consequently, this mapping of

degradation hotspots is different from, indeed not as contentious as, the production of an accurate map of all degraded areas.

2. Literature Review

Land degradation is a major global problem. There have been many efforts to map land degradation at global and regional scales (Dregne, 1977; Oldeman *et al.*, 1990; USDA-NRCS, 1998; Eswaran *et al.*, 2001; Herrmann *et al.*, 2005; Wessels *et al.*, 2007; Bai *et al.*, 2008b; Hellden and Tottrup, 2008; Hill *et al.*, 2008; Vlek *et al.*, 2008; Vlek *et al.*, 2010; Le *et al.*, 2012; Bai *et al.*, 2013; Conijn *et al.*, 2013; Dubovyk *et al.*, 2013). However, despite these efforts, the existing global maps of land degradation are weakened by serious shortcomings. The earlier mapping exercises used subjective expert opinion surveys as the basis for the maps, with unknown direction and magnitudes of measurement errors. The more recent of these studies are making use of now globally available remotely-sensed NDVI data (Tucker *et al.*, 2005), but NDVI also has its own shortcomings as a proxy for land degradation, such as various confounding effects (Pettorelli *et al.*, 2005). These include: (1) remnant cloud-cover effects in humid tropics; (2) soil moisture in sparse vegetative areas, which reduces the NDVI signal, (3) seasonal variations in vegetation phenology (proportional with weather seasonality) and time-series autocorrelation; (4) site-specific effects of vegetation structure and site conditions (e.g. topography and altitude). These confounding effects can be mitigated at some degree, but not completely removed. As a consequence, NDVI trend is always affected by unexpected noise, thus bearing considerable uncertainty in a way that where there are small magnitudes of NDVI trend, the risk that errors/noises in the NDVI data are larger than the trend itself is much higher (Tucker *et al.*, 2005).

Moreover, there are major factors confounding the relationship between NDVI (NPP) trend and human-induced land degradation. These confounding effects include: (1) the effect of inter-annual rainfall variation on NDVI (NPP) (Herrmann *et al.*, 2005), (2) the effect of atmospheric fertilization on vegetation greenness and growth (Boisvenue and Running, 2006; Reay *et al.*, 2008; Lewis *et al.*, 2009; Buitenwerf *et al.*, 2012; Le *et al.*, 2012), and (3) intensive uses of chemical fertilizers in intensified croplands (Vlek *et al.*, 1997; Potter *et al.*, 2010; MacDonald *et al.*, 2011). The biomass productivity of the land is often a low priority

service in many urbanized areas, where space provision is usually the most expected service of the land.

To isolate human-induced biomass production decline from the one driven by rainfall, currently, there are different methods: residual trend analysis method (*ResTrend*) (Evans and Geerken, 2004; Herrmann *et al.*, 2005) (Wessels *et al.*, 2007), the trend-correlation stepwise method (*Trend-Correlation*) (Le et al., 2012; Vlek et al., 2010), or trend-correlation with the additional use of rain-use efficiency (RUE) (Bai *et al.*, 2008a; Fensholt *et al.*, 2013). The first two methods use the correlation between inter-annual NDVI and rainfall data for isolating pixels with biomass production decline not caused by rainfall inter-annual variation. If there is no other natural drivers of biomass production decline besides the reduction of annual rainfall, the biomass production decline in these pixels is likely caused by human activities. The comparisons between the uses of two methods at global level (Dent *et al.*, 2009) and national level (Vu *et al.*, 2013) showed similar results. While rain-use efficiency has been recently used in some land degradation assessments in dry lands (Wessels *et al.*, 2007; Fensholt *et al.*, 2013), there are concerns about the use of rain-use efficiency for continental and global scale (Dent *et al.*, 2009), especially in the humid tropics where rainfall is generally not a limited factor of primary productivity.

The effect of atmospheric fertilization caused by elevated levels of CO_2 and NO_x in the atmosphere (Dentener, 2006; Reay *et al.*, 2008) complicates the global assessment of land degradation using the NDVI-based approach. Increased atmospheric fertilization (AF) can cause a divergence between greenness trend and soil fertility change as the fertilization effect has not been substantially mediated through the soil. The rising level of atmospheric CO_2 stimulates photosynthesis in plants' leaves, thus increasing NPP, but the soil fertility may not necessarily be proportional with the above ground biomass improvement. The wet deposition of reactive nitrogen and other nutrients may affect positively plant growths as foliate fertilization without significantly contributing to the soil nutrient pool, or compensating nutrient losses by soil leaching and erosion. Global observations, both field measurements (Boisvenue and Running, 2006; Lewis *et al.*, 2009; Buitenwerf *et al.*, 2012) and remotely sensed data analyses (Vlek *et al.*, 2010; Fensholt *et al.*, 2012; Le *et al.*, 2012) show long-term improvement of biomass productivity in large areas that cannot be attributed to either human interventions or rainfall improvement. In Africa, the biomass

increased at a rate of 0.63±0.31 Mg ha^{-1} yr^{-1} over the past 4 decades for closed-canopy tropical forest sites with ample rain and free of human interventions (Lewis *et al*., 2009).

As NDVI values can be affected by several site- and land cover- specific factors (Pinter *et al.*, 1985) (Markon *et al.*, 1995; Thomas, 1997; Mbow *et al.*, 2013), different locations with the same NDVI value are not necessarily have the same biomass productivity. Thus, comparison of biomass productivity between pixels using NDVI is a pitfall that should be avoided (Pettorelli et al., 2005). Recent studies suggested interpreting the NDVI trend results for each spatial stratum of social-ecological conditions in order to gain more insights about likely degradation processes and affecting factors in the delineated hotspots (Vlek *et al.*, 2010; Sommer *et al.*, 2011; Le *et al.*, 2012; Vu *et al.*, 2014). Because land use/cover refers to ecosystem exploitation (Nachtergaele and Petri, 2008) and is conditioned by several anthropogenic factors that define the social and ecological contexts for interpreting causalities from statistical results, broad land-use classes have been recommended for stratifying causal analyses and interpretations of land degradation (Vlek *et al.*, 2010; Sommer *et al.*, 2011; Vu *et al.*, 2014).

3. The Conceptual Framework

In this study, "land degradation" is understood in a broad sense. From internationally authoritative concepts of United Nations Convention to Combat Desertification (UNCCD, 2004) and Millennium Ecosystem Assessment (MEA, 2005), ***land degradation is defined as the persistent reduction or loss of land ecosystem services, notably the primary production service*** (Safriel, 2007; Vogt *et al.*, 2011). The aspects emphasized in this definition of land degradation include:

- First, "land" is understood as a terrestrial ecosystem that includes not only soil resources, but also vegetation, water, other biota, landscape setting, climate attributes, and ecological processes (MEA, 2005) that operate within the system, ensuring its functions and services.

- Second, the definition focuses on the ecological services of the land: land degradation makes sense to our society only in the context of human benefits

derived from land ecosystems uses (Safriel, 2007). Negative changes in soil component (e.g., soil erosion, deteriorations of physical, chemical, and biological soil properties) are concerned as much as how serious these changes result in reductions of supporting (e.g., primary production), provisioning (e.g., biological products including foods) and regulating (e.g., carbon sequestration) services of the land (i.e., land ecosystem).

- As a consequence, the definition emphasizes the pivotal role of primary production among a wide range of land's services. The crucial reason for this emphasis is that primary production generates products of biological origin, on which much of other ecosystem services depend (Safriel, 2007). The primary production is the basis of food production, regulates water, energy, and nutrient flows in land ecosystems, sequestrates carbon dioxide from the atmosphere and generally provides habitats for diverse species (MEA, 2005).

4. Methodology and Data

The methodological approaches applied in this study build on this previous literature and, in fact, seek to address some of the shortcomings of the previous research on global land degradation hotspots mapping.

4.1 Proxy indicator approach to mapping of degradation hotspots

In the context of land degradation hotspots mapping, land degradation proxies (i.e., key indicators that approximate relevant processes of land degradation) are often used to delineate degradation hotspots. Although using proxies of land degradation is always prone to considerable uncertainties, the proxy method is relevant for mapping global, continental and national degradation hotspots due to the following reasons:

- The main target is the areas with high magnitude and extent of degradation, i.e., where temporal and spatial variations of the used proxies are high and observable. This helps mitigate the adverse effects of the inherently high uncertainty of the used proxies (Vu et al., 2013). The lower is the temporal and spatial variation of the used proxies, the lower is the relevance of the proxy method.

- The considered scale is global, or continental or national and the related need is to delineate degradation hotspot at coarse resolution (e.g., 1 - 10 km) (Vogt et al., 2011).

- There are no other data alternatives for long-term (> 2 decades), large scale (global or continental) assessments (Vlek et al., 2010; Fensholt et al., 2012).

- Efforts to improve global/continental land degradation assessment require the first version of a global land degradation map to guide where and what needed to be verified in the next steps.

4.2 Long-term trend of annual NDVI as the proxy of long-term biomass productivity decline

Given the global scale and long-term perspectives of the study, we used the long-term trend of inter-annual mean Normalized Difference Vegetation Index (NDVI) over the period 1982–2006 as a proxy for a persistent decline or improvement in the Net Primary Productivity (NPP) of the land, thereby delineating past land degradation hotspots. This NDVI-based assessment of land degradation has been used by many studies (Bai *et al.*, 2008b; Hellden and Tottrup, 2008; Vlek *et al.*, 2010; Le *et al.*, 2012). However, as we highlighted in the literature review, NDVI as a proxy for land degradation has several caveats. Our strategy to address these caveats in this NDVI-based mapping of land degradation hotspots is summarized in Table 1.

Table 1. Measures for mitigating or correcting confounding effects in the presented NDVI-based mapping of land degradation hotspots.

Confounding factors	Affected relationship or process	Mitigating/correcting measure used in this study	Done/advised by other studies
Remnant cloud-cover effect in humid tropics	NDVI vs. NPP weakened	Only non-flagged pixels used (2)*	(Tucker *et al.*, 2005; Brown *et al.*, 2006)
Effect of soil moisture in sparse vegetative areas	NDVI vs. NPP weakened	Eliminating pixel with NDVI < 0.05, arid zone; cautions in sparse vegetation areas (2)*	(de Jong *et al.*, 2012; Fensholt *et al.*, 2012; Le *et al.*, 2012)
Seasonal variations in vegetation phenology and time-series autocorrelation	Inter-annual NDVI (NPP) trend confounded	Use annually average NDVIs instead of bi-weekly or monthly NDVIs (1)*	(Bai *et al.*, 2008b; Hellden and Tottrup, 2008; de Jong *et al.*, 2011; de Jong *et al.*, 2012)
Site-specific effects of vegetation/crop structure and site conditions	NDVI vs. NPP weakened	No spatial trend of NDVI used (3)* Land-use/cover-specific interpretation (6)* Eliminate/cautious with area having LAI > 4 (6)*	(Pettorelli *et al.*, 2005) (Vu *et al.*, 2014) (Carlson and Ripley, 1997; Vu *et al.*, 2013)
Larger errors /noises in the NDVI data compared to the small NDVI trend itself	Not reliable Inter-annual NDVI (NPP) trend	Not consider pixels with no statistic significance or very small magnitude of NDVI trend (e.g., < 10% / 25 years) (3)*	(Le *et al.*, 2012; Vu *et al.*, 2014)
Effect of inter-annual rainfall variation on NDVI (NPP)	Mixture between climate-driven and human-induced NPP trend	Correct partly rainfall effect by consider NDVI-rainfall correlation (4)*	(Herrmann *et al.*, 2005; Bai *et al.*, 2008b; Le *et al.*, 2012)
Effect of atmospheric fertilization (AF) on NDVI (NPP)	Mixture between climate-driven and human-induced NPP trend	Correct partly AF effect by consider NPP growth in pristine areas (5)	(Le *et al.*, 2012)
Effect of intensive fertilizer uses on NDVI (NPP)	Mixture between fertilizer-driven NPP soil-based NPP	Masking areas with high fertilizer use for follow-up study (7)	
Irrelevance of considering NPP in urbanized areas	NPP is not relevant indicator	Masking urban areas from the consideration (2)	(Le *et al.*, 2012; Vu *et al.*, 2014)

Note: *= number within parentheses indicates the related step in Fig. 1

The procedure of the analytical flow is shown in Figure 1. The detailed explanations of major analysis steps are given in the corresponding results sections for better contextual understanding.

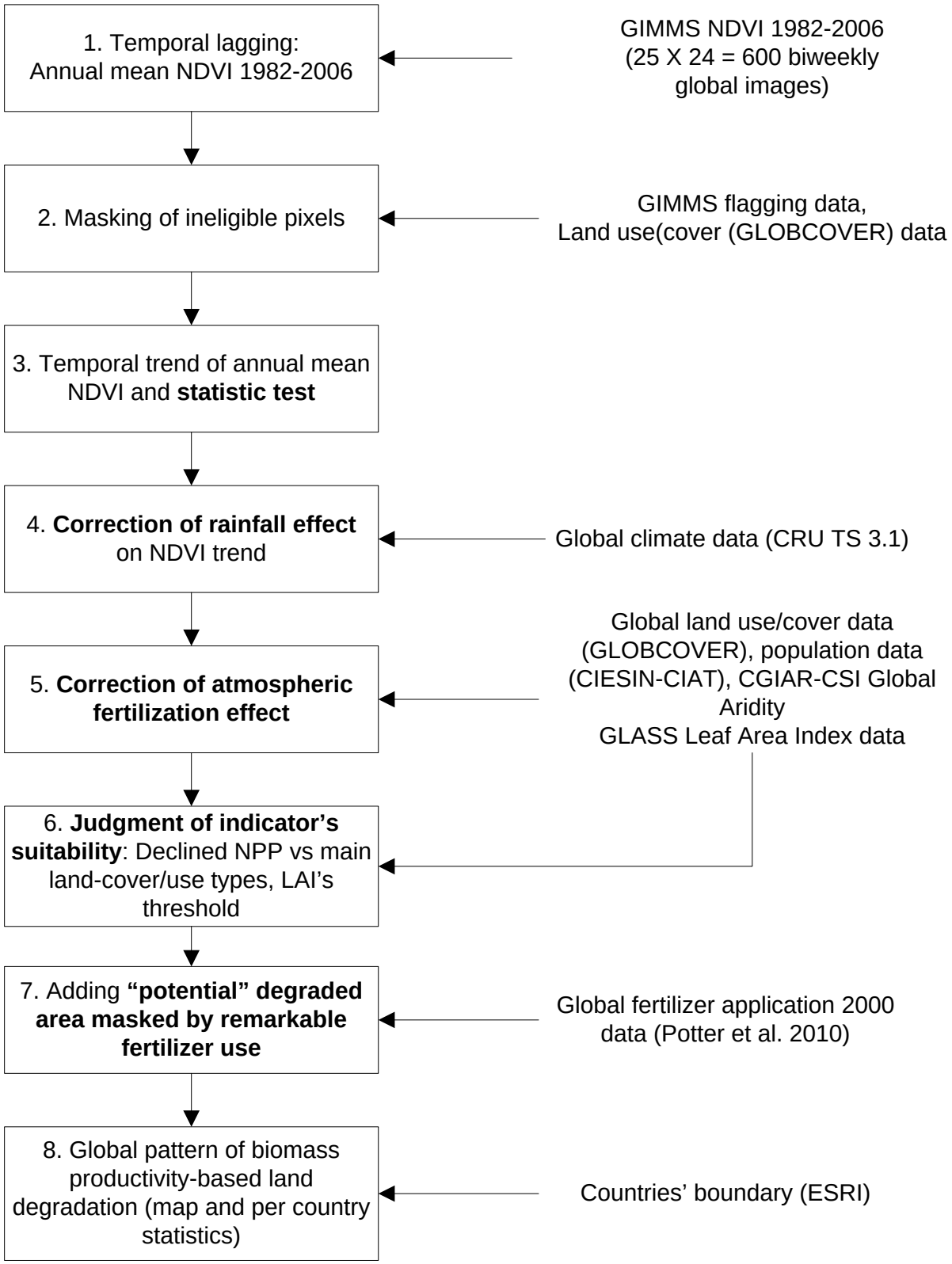

Figure 1. Procedure of biomass productivity-based assessment of NDVI.

Note: The bold text indicates relatively new features compared to previous studies.

GIMMSg-NDVI data

The employed dataset of vegetation index Global Inventory Modeling and Mapping Studies (GIMMS) Satellite Drift Corrected and NOAA-16 incorporated Normalized Difference Vegetation Index (NDVI), Monthly 1981–2006, is called GIMMSg-NDVI dataset. This dataset is available for free at the Global Land Cover Facility (GLCF), the University of Maryland (GLCF - http://glcf.umiacs.umd.edu/data/gimms/ -accessed in 01 May 2013).

This GIMMSg-NDVI version is selected for analysis because of the following reasons:

- For global land degradation assessment over long terms, there may be no other alternative data. At present the GIMMS-NDVI data archive is the only global coverage dataset spanning 1982 to recent time.

- The NDVI dataset was calibrated and corrected for view geometry, volcanic aerosols, and other effects not related to vegetation change (Pinzon *et al.*, 2005; Tucker *et al.*, 2005). As a result, this new GIMMS NDVI dataset, used in this study, is relatively consistent over time and is of higher quality compared to the previous versions produced by the GIMMS group (Brown *et al.*, 2006). Using Terra MODIS NDVI as a reference (Fensholt *et al.*, 2009) in Sahel region found that the GIMMS NDVI data set is well-suited for long term vegetation studies of the Sahel–Sudanian areas.

- The GIMMSg-NDVI archive "should provide a large improvement over previously used NDVI data sets, because the data are collected by one series of instruments, and they give a more realistic representation of the spatial and temporal variability of vegetation patterns over the globe" (GLCF, accessed in 01 May 2013).

- Validity of the GIMMS dataset has been discussed in previous studies (Tucker *et al.*, 2005; Brown *et al.*, 2006), and is subjected to ongoing validation (Fensholt *et al.*, 2012; GLCF, accessed in 01 May 2013).

The full list of data sources used is given in Annex 1.

5. Results

5.1 Aggregating annual mean NDVI time-series (1982-2006) (Step 1 in Figure 1)

To minimize the confounding effects of seasonal variations and time-series autocorrelation, we used annual average NDVI instead of the original bi-weekly GIMMS NDVI time-series, which is similar to Hellden and Tottrup (2008) and Vlek *et al.* (2010). This treatment is supported by the recent findings of de Jong *et al.* (2011). They found that inconsistencies between the linear trends of annually aggregated GIMMS NDVI and the seasonality-corrected, non-parametric trends of the original GIMMS NDVI time-series (biweekly) were mainly on areas with weak or non-significant NDVI trends, which are not central in our hotspot approach. The year 1981 was excluded because it has only data for the later 6 months (July-December). As a result, there are 25 annual mean NDVI images calculated from 600 original GIMMSg images.

5.2 Masking ineligible pixels (Step 2 in Figure 1)

As explained in Table 1, pixels with the following statuses were masked from the course of the analyses:

- To partly avoid the effect of cloud cover or cloud shade, flagged GIMMS pixels, i.e., flag > 0 indicates a not good value of NDVI, were masked.
- As NDVI is not a suitable indicator of NPP in bare, or very sparse vegetation, pixels with NDVI < 0.05 were masked.
- Pixels with bare surface, urban and industrial areas, based on GLOBCOVER version 2.2 data (Bicheron *et al.*, 2008), were masked.

Figure 2 depicts the resulting global pattern of the average annual mean NDVI over 1982-2006 on the eligible (non-grey) areas.

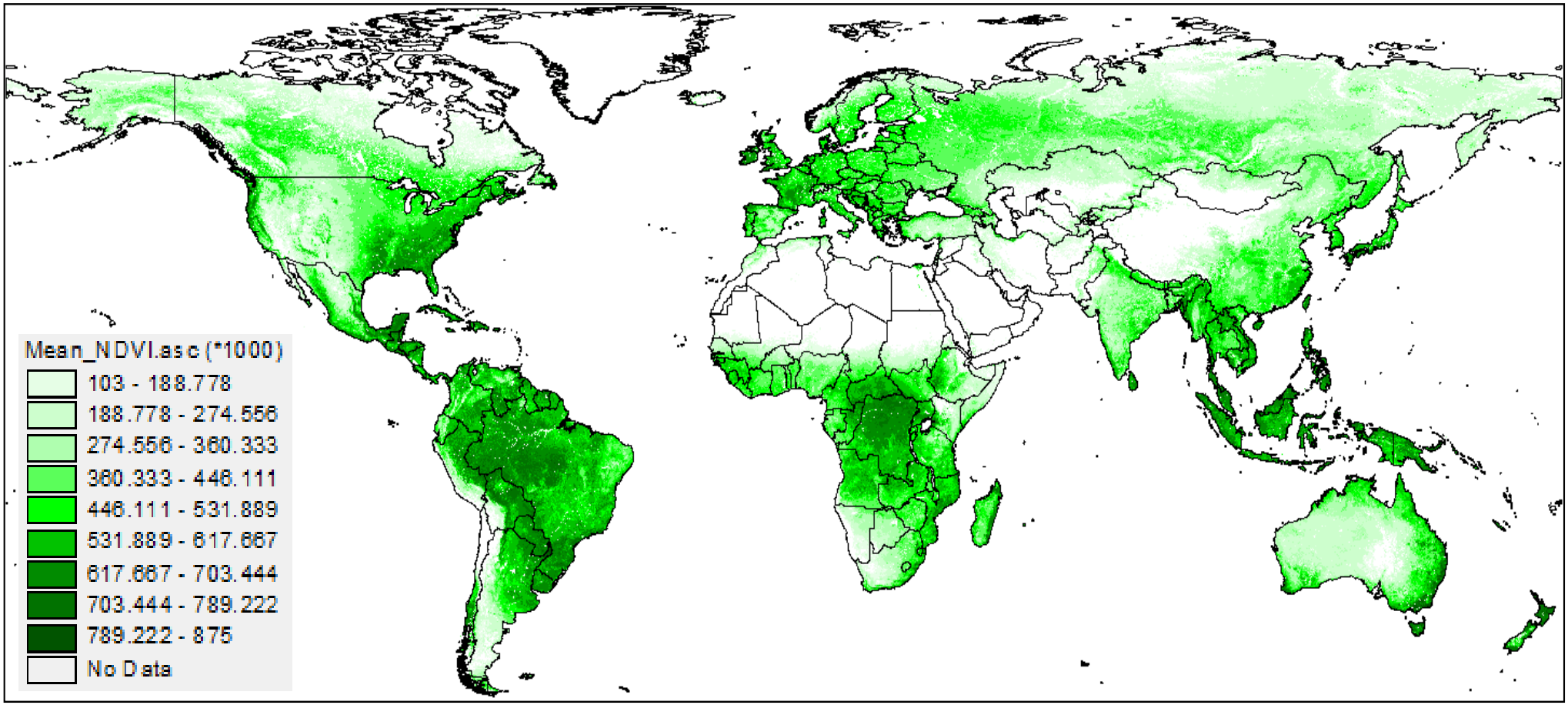

Figure 2. Average annual mean NDVI (scale factor = 1000) of the period 1982-2006.

5.3 Significant trend of annual mean NDVI over 1982-2006 (25 years) (Step 4 in Figure 1)

Temporal slope metrics and statistical test

For each pixel *i*, the long-term trend of annual NPP (via vegetation index) can be formalized by the slope coefficient (A_i) in the simple linear regression relationship

$$V_i = A_i \times t + B_i \qquad (1)$$

where V_i = annual mean NDVI, A_i = long-term trend of NDVI, t = year (elapsing from 1982 to 2006), B_i = intercept (an indicator for a possible delay in the onset of degradation). The computed slope coefficient *A* for each pixel was tested for statistical significance at different confidence levels at 90% (*P <0.1*), which is sufficient for long-term trend analyses of noisy parameters like NDVI (Le *et al*. 2012; Vlek *et al*. 2010).

Figure 3 shows the significant trend in a statistical manner only. A statistically significant trend can be with a too small magnitude that can be either not significant in practice, or lower than errors/noises in NDVI time-series. Both cases should not be meaningful for consideration. Thus, it is much more meaningful to look at the relative change in inter-annual NDVI compared to the period mean (in Figure 2).

Significant biomass productivity decline

Significant biomass productivity (annual mean NDVI) decline is defined by the following criteria:

- Negative NDVI slope with a statistical significance ($p < 0.1$), and
- Meaningful magnitude of the NDVI decline: relative NDVI annual reduction ≥ 10% / 25 years (or ≥ 0.4% / year) (Vlek *et al*., 2010; Le *et al*., 2012; Vu *et al*., 2013). There are two reasons for selecting this cut-off threshold. First, from a common sense, a reduction rate of less than 0.4 - 0.5% per year can be considered to be insignificant in practice. Second, with these very small magnitudes of NDVI trend, the risk that inherent errors/noises in the NDVI data are larger than the trend itself is high, making the NDVI trend less reliable (Tucker *et al*. 2005). This cut-off value helps avoid that risk.

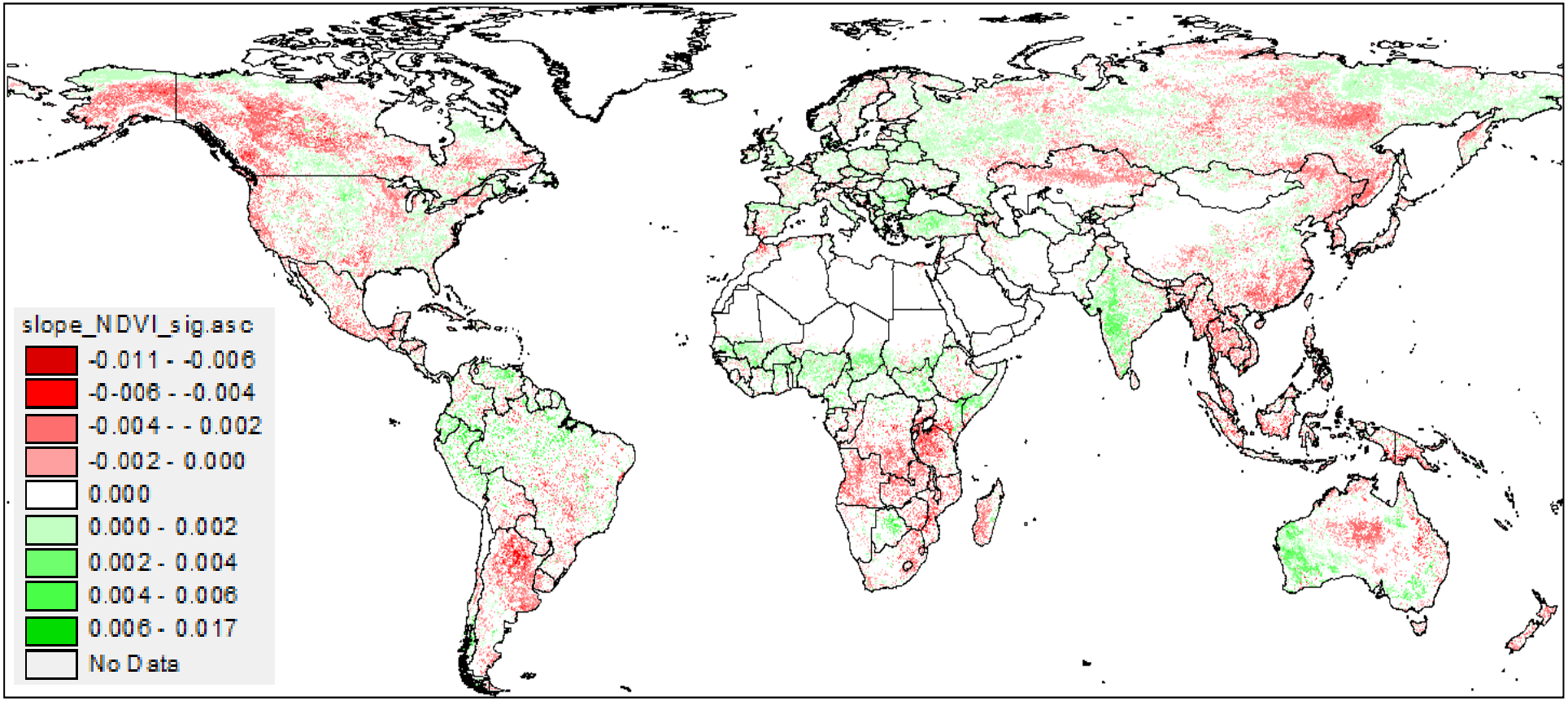

Figure 3. Significant ($p < 0.1$) slope of inter-annual NDVI over 1982-2006.

Notes: White areas are with either no data, or statistically non-significant trend. There has been no minimal threshold of NDVI slope applied yet

Figure 4 shows spatial pattern of annual decline of biomass productivity in percentages of the period mean of NDV (Fig. 4a) and in the dummy scale (i.e., 1= significant productivity decline, 0= otherwise) (Fig. 4b).

a)

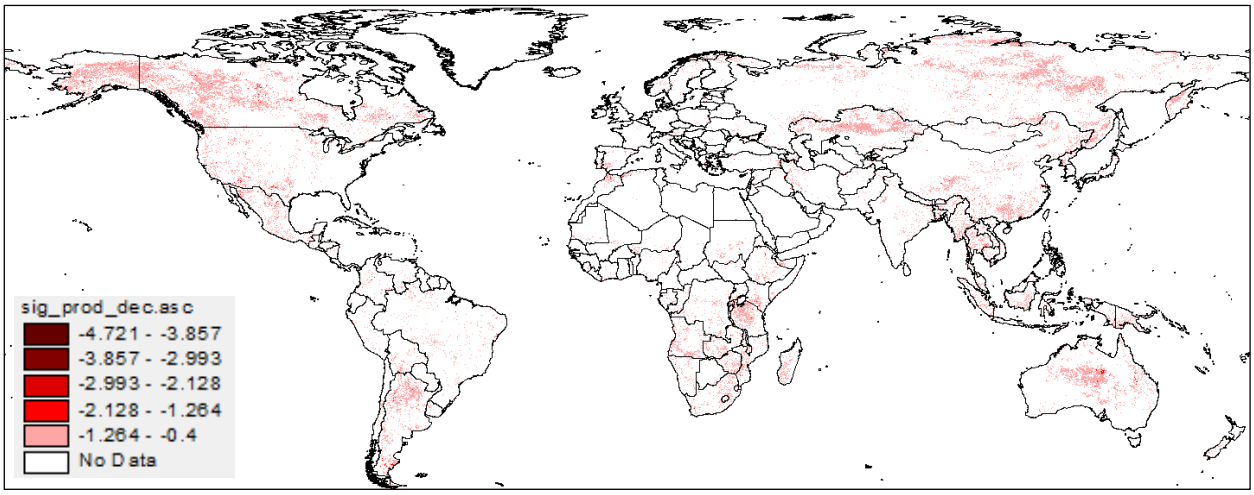

b)

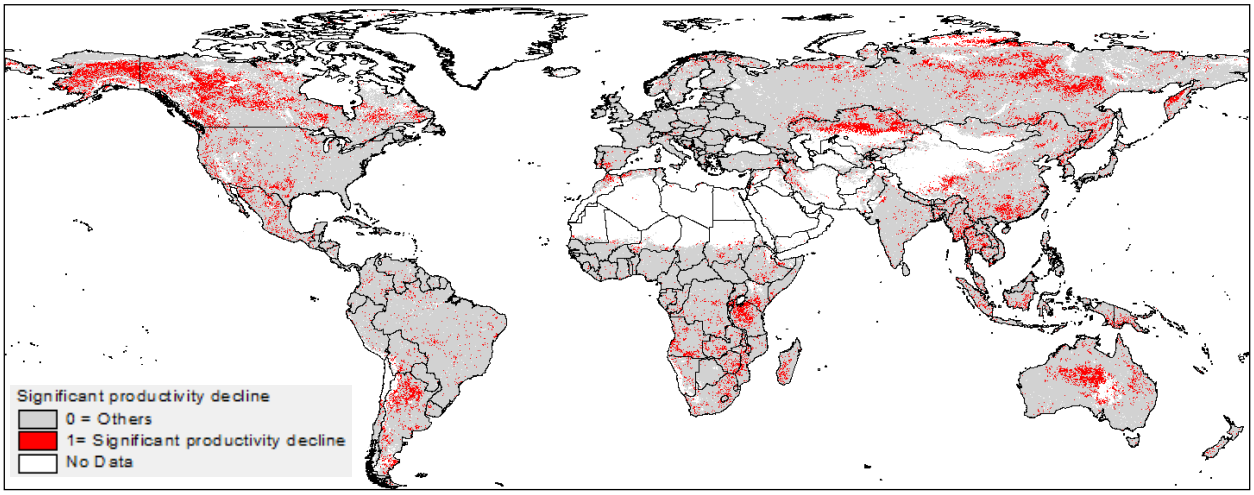

Figure 4. Significant ($p < 0.1$ and reduction rate ≥ 10% / 25 yrs) biomass productivity decline over 1982-2006.

a) Annual reduction rate (% of period mean), b) dummy scale (area of significant productivity decline = 15,336,128 km^2)

5.4 Correction of rainfall variation effect

The significant decline of inter-annual NDVI shown in Figure 4 can be attributed to either temporal variation in rainfall or human activities (e.g., land cover/use conversion and/or change in land use intensity).

The annual rainfall data for the period 1982–2006, which was extracted from the TS 3.1 dataset of the Climatic Research Unit (CRU) at the University of East Anglia (UK), were used for the isolating purpose. The original data include grids of monthly rainfall data at a spatial resolution of 0.5°, covering the 1901–2006 period (Mitchell and Jones, 2005). To match the spatial resolution of AVHRR-NDVI data for later analysis, the grid cells of rainfall data were re-sampled to match with the 8-km resolution of NDVI data, using nearest neighbour statistics.

The *Trend-Correlation* method is used to account for rainfall variation effect. The procedure of *Trend-Correlation* method (Vlek *et al*., 2010) involves:

- For each pixel, Pearson's correlation coefficient between inter-annual NDVI and rainfall over the 1982–2006 period (R_i) is calculated.
- The statistical significance for pixel-based correlation coefficients at a confidence level of 95% ($p < 0.05$) is tested.
- A pixel was considered to have a strong correlation between its inter-annual NDVI and rainfall if the correlation coefficient was significant ($p < 0.05$) and greater than 0.5 or lower than -0.5.
- If the pixel has a significantly negative NDVI trend (negative A_i, $p < 0.1$) and a strongly positive vegetation–climate correlation ($R_i > 0.5$; $p < 0.05$), the NDVI decline at the location was determined by the rainfall factor. Otherwise, the NDVI decline was likely caused by non-climate factors.

The limitation of the method is that in the pixels with significantly negative NDVI trend and positive vegetation–rainfall correlation (or non-significant residue trend in *ResTrend* method), both rainfall and human effects can be mutually exclusive. The elimination of these pixels may also exclude some human-induced degradation areas.

The long-term response of inter-annual NDVI to rainfall variation is shown in Figure 5. Then, the NDVI decline pattern from which rainfall-driven pixels were masked is given in Figure 6.

a)

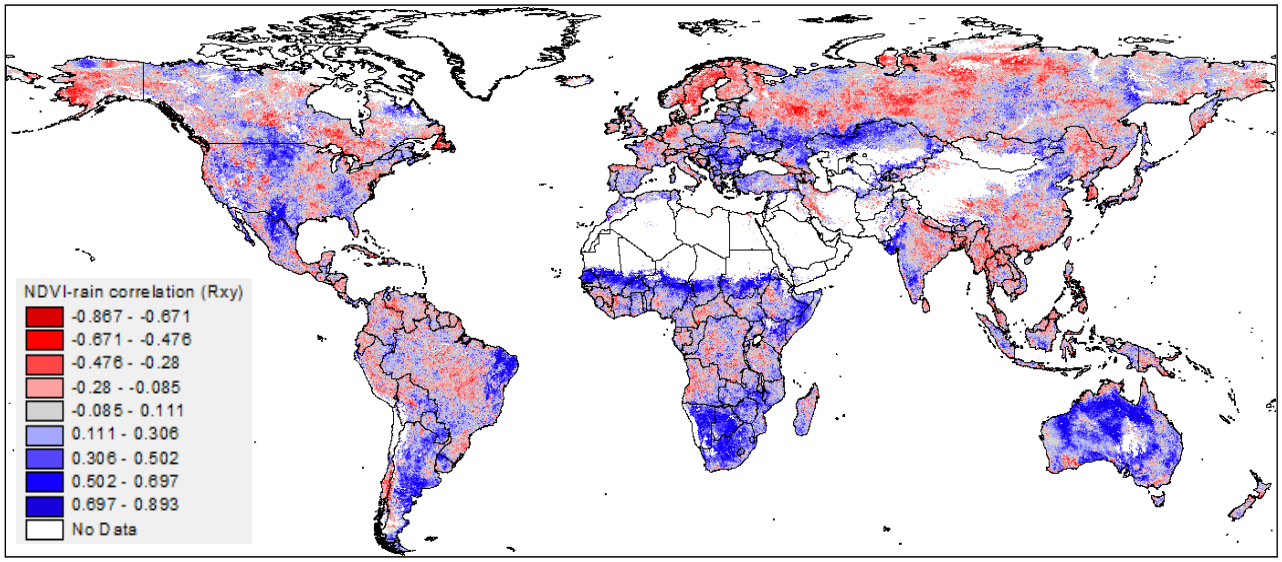

b)

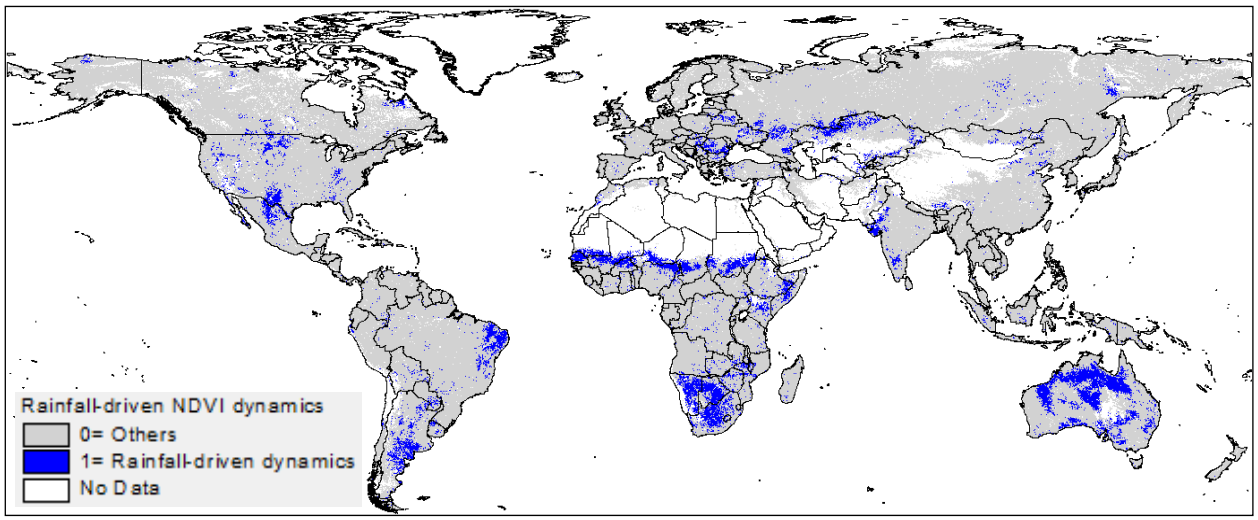

Figure 5. Long-term response of inter-annual NDVI to rainfall variation (1982-2006): a) correlation coefficient (R_{xy}) between inter-annual NDVI and rainfall, b) area of rainfall-driven NDVI dynamics ($p < 0.05$ and $R_{xy} \geq 0.5$) that was masked from further analysis (masked area in blue = 10,654,464 km^2).

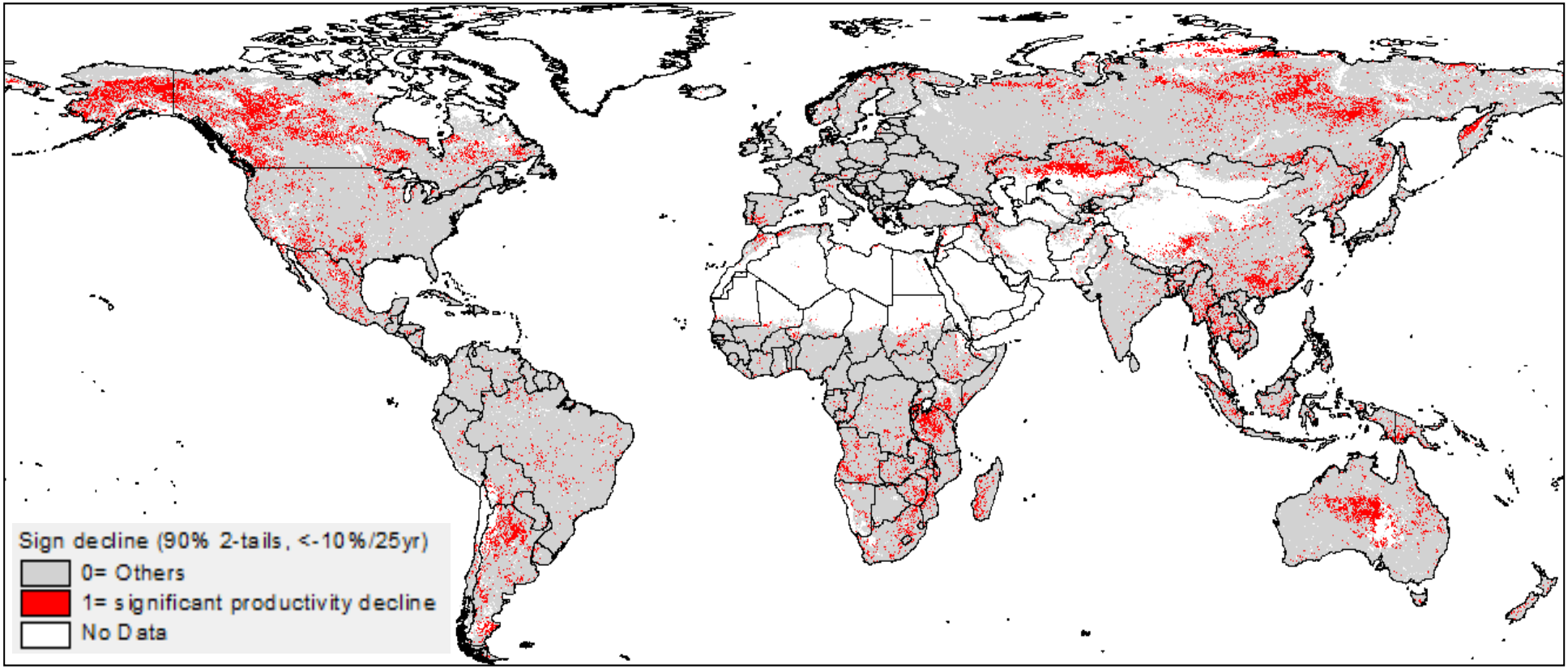

Figure 6. Significant ($p < 0.1$ and reduction rate ≥ 10% / 25 yrs) biomass production (NDVI) decline corrected for rainfall effect (area in red = 14,525,952 km^2).

Based on the map in Figure 6, the total land with significant biomass production decline ($p < 0.1$, reduction rate ≥ 10%/25 yrs) corrected for rainfall effect is about 14.5 million km^2, or about 10 % of the total global land area (i.e., 226,968 pixels, or 14,525,952 km^2).

5.5 Correction of atmospheric fertilization effect (Step 5 in Figure 1)

Calculate the sub-component of AF-driven growth

The actual change in vegetation productivity can be considered the net balance between the partial changes caused by human activities and those caused by natural processes (i.e., effects of rainfall and/or AF). In pristine vegetative areas, actual vegetation dynamics can be driven by only natural drivers as the human-induced component of biomass dynamics can be assumed to be zero. If these areas, in addition, have no correlation between biomass productivity and weather parameters, weather effects can be neglected and the actual growth can be assumed to be caused by atmospheric fertilization (Vlek *et al*., 2010). Thus, *the quantum of AF-driven growth of a particular vegetation type can be found in the pristine (no significant human disturbance) areas of that type with no NDVI-rainfall correlation.*

We defined the above-mentioned areas by applying an overlaying scheme as shown in Figure 7.

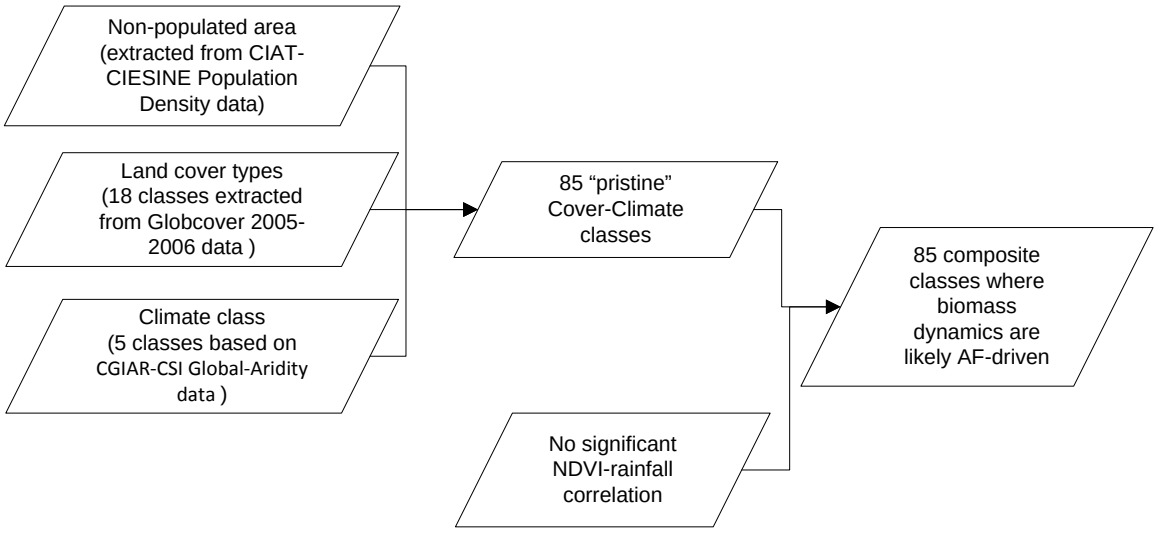

Figure 7**. Overlaying scheme for defining areas of pristine (no significant human disturbance) vegetation with no NDVI-rainfall correlation, where biomass dynamics are likely AF-driven.**

As a result, we identified 246,159 pixels (i.e., 15,754,176 km^2) belonging to 85 'pristine' (no significant human disturbance) Cover-Climate types that are all with no significant NDVI-rainfall correlation (see Figures 7 and 8). As explained, vegetation biomass dynamics in these areas are likely driven by atmospheric fertilization (AF) effect.

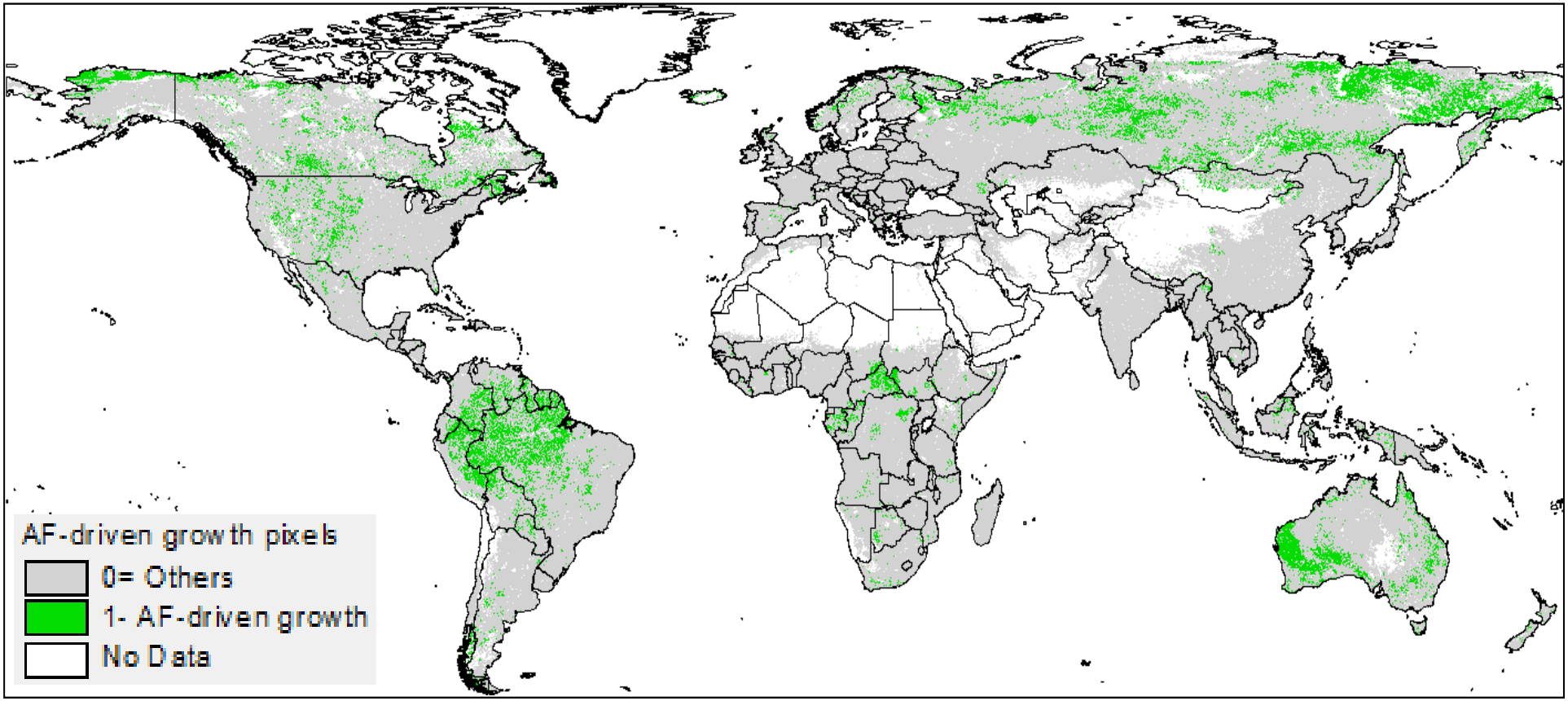

Figure 8. Spatial pattern of pristine vegetation with no NDVI-rainfall correlation where biomass dynamics are likely AF-driven (area in green = 15,754,176 km^2).

The correction of AF effect was then done by three steps:

- Calculate means of NDVI slope for each Cover-Climate-No Correlation types: $dNDVI_{AF,k,}/dt$ where *k* indexes the Cover-Climate type.

- Re-calculation of AF-adjusted inter-annual NDVI time-series through subtracting the NDVI data by quantum $dNDVI_{AF,k,}/dt$. This re-calculation of NDVI time-series was specific for each Cover-Climate class *k*, i.e. AF-driven NDVI accrual for each class was used for recalculation of NDVI time-series on elsewhere with the same class

  $NDVI_{AF\text{-}adjusted,\ 1983,\ k} = NDVI_{1882,k} - 1 * dNDVI_{AF,k,}/dt$

  $NDVI_{AF\text{-}adjusted,\ 1984,\ k} = NDVI_{1882,k} - 2 * dNDVI_{AF,k,}/dt$

  $NDVI_{AF\text{-}adjusted,\ 1985,\ k} = NDVI_{1882,k} - 3 * dNDVI_{AF,k,}/dt$

  ....

  $NDVI_{AF\text{-}adjusted,\ 2006,\ k} = NDVI_{1882} - 24 * dNDVI_{AF,k,}/dt$

- Re-calculate the trend of inter-annual AF-adjusted NDVIs, test the statistical significance of the trend, and calculate $NDVI_{AF\text{-}adjusted}$ - Rainfall correlation.

The AF-corrected significant biomass productivity decline is showed in Figure 9a (in % of period-mean $NDVI_{AF\text{-}adjusted}$) and 9b (in dummy scale). There are 633 443 pixels, i.e., 40 540 352 km^2 of global land (i.e. 27%) likely to have experienced significant biomass productivity decline given that the effects of rainfall and atmospheric fertilization are taken into account.

5.6 Identification of areas with saturated NDVI zone and relation to land-use/cover strata (Step 6 in Figure 1)

The NDVI-vegetation productivity relationship can be saturated, thus biased in areas with dense vegetation canopies (Pettorelli *et al.*, 2005). In the areas having dense vegetation with Leaf Area Index (LAI) more than 4, the relationship between NDVI and the vegetation biomass tends to be saturated (i.e., NDVI is less sensitive to actual biomass change), thus should be used with special cautions (Carlson and Ripley, 1997).

a)

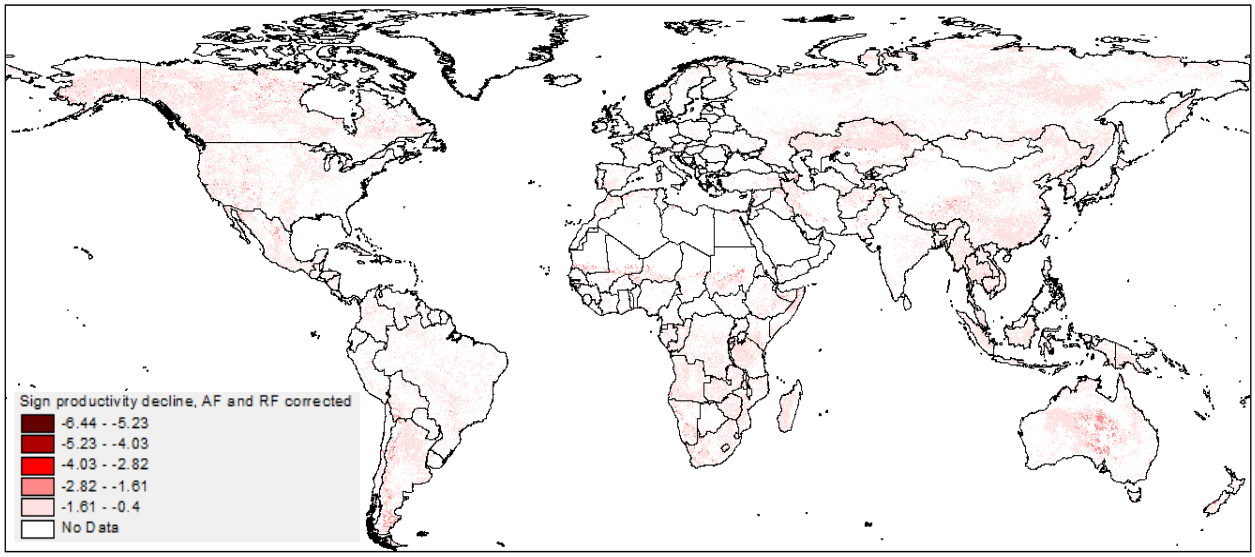

b)

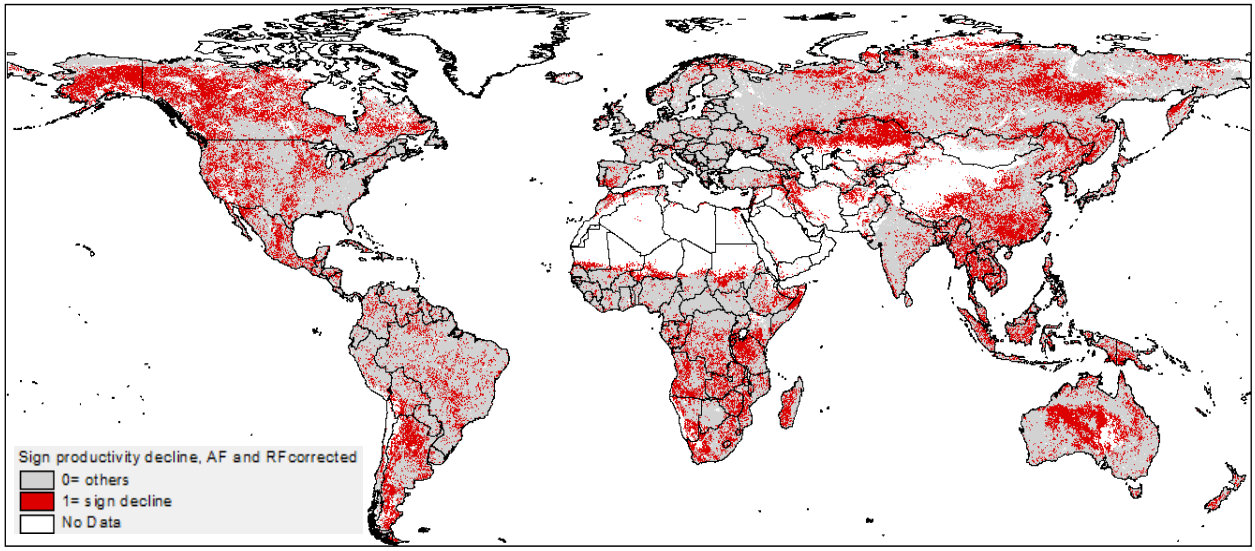

Figure 9. Significant productivity decline with correction for both atmospheric and rainfall effects: a) relative annual rate, b) dummy scale (area in red = 40,540,352 km^2).

We calculated the mean annual LAI of the period 1982 - 2006 by using the GLASS LAI dataset (Liang and Xiao, 2012; Xiao *et al.*, 2014). To avoid the computational abundance (each year has 46 8-day LAI images), we calculated the mean of 8-day LAI in representative years 1985, 1990, 1995 and 2000 (i.e., n = 46 x 4 = 184 global images taken into account).

a)

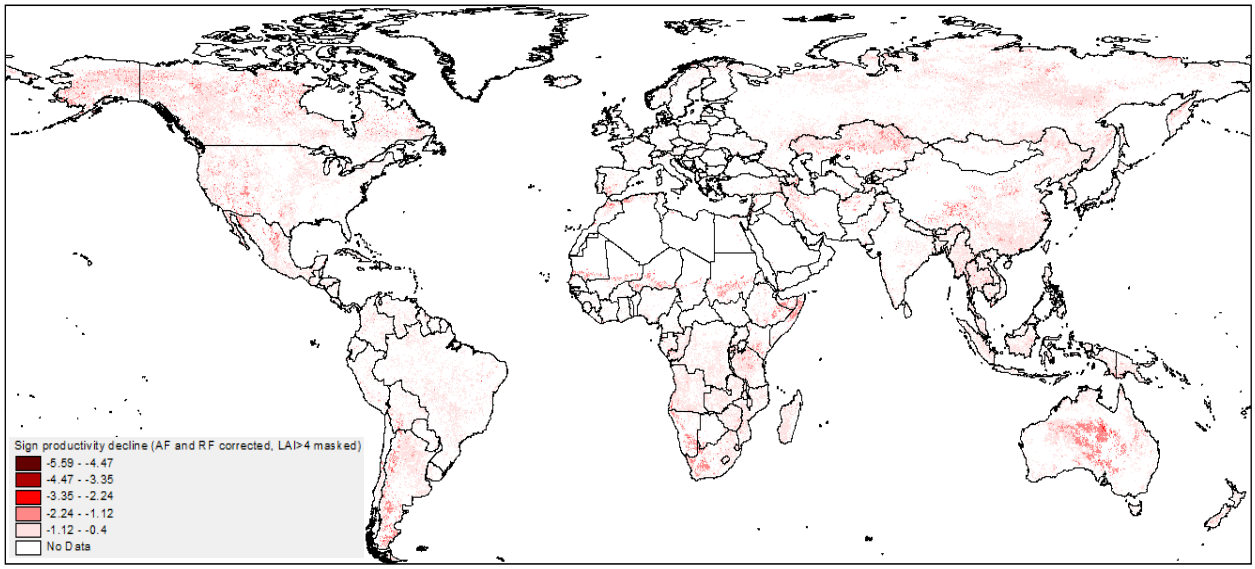

b)

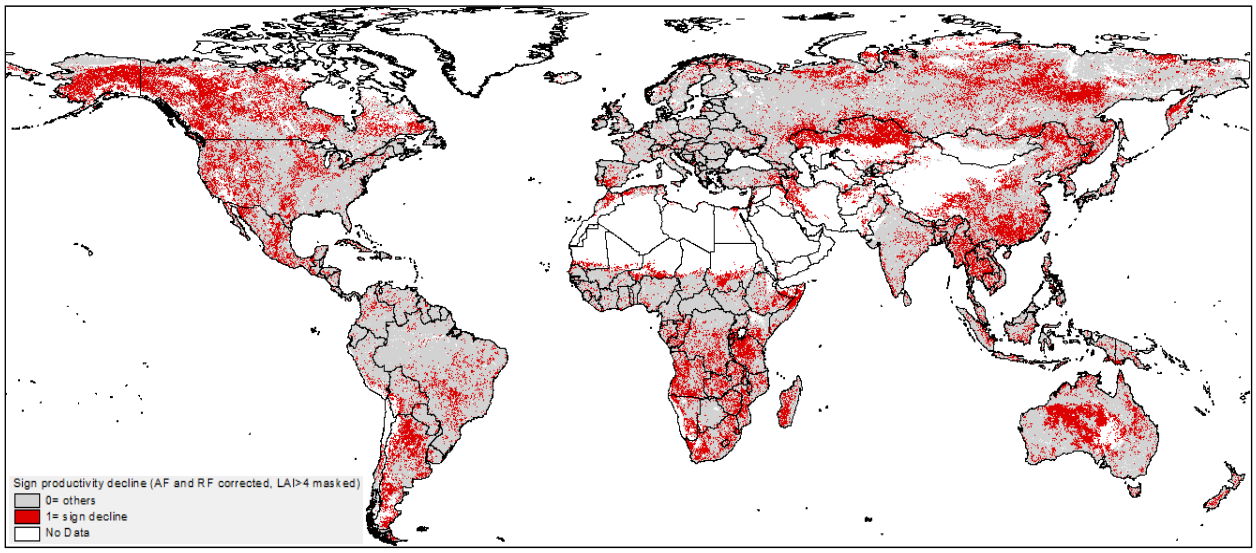

Figure 10. Significant productivity decline with correction for rainfall and atmospheric fertilization effects and masking of NDVI-saturated pixels. a) relative annual rate, b) dummy scale (area in red = 35,948,032 km^2)

As a result, of 633 443 declined pixels in Figure 9 there are 71 755 pixels (11%) with LAI > 4 possibly making their NDVI trend not reliable for indicating vegetation biomass productivity. Land degradation in these NDVI-saturated pixels should be considered with other indicators, rather than NDVI signals. Given the NDVI-saturated pixels masked, the area of biomass productivity decline is about 36 million km^2 , i.e. 24% of global land area. These areas are shown in Figure 10a (in % of period-mean $NDVI_{AF\text{-}adjusted}$) and 10b (in dummy scale).

The map in Figure 10a shows that most of NDVI degrading areas have small annual reduction magnitude (i.e. less than 1% / year, as showed in the area in pink). Given the inherently high noise of NDVI signal, uncertainty of the calculated degrading trend in these pink areas can be higher than the pixels with higher annual NDVI reduction rate, i.e. the red to dark red pixels in Figure 10a.

5.7 Relation to land cover strata

At the resolution of this global study (i.e., 8-km pixel), many sub-classes of scattered land cover/use (e.g. slash-and-burn field, mountain paddy rice terraces and fruit plantations) will be dissimulated. Thus, we used 7 broad land use/cover classes (see Figure 11) aggregated from 23 classes of the Globcover 2005-2006 data (Bicheron *et al.*, 2008). The spatial pattern of long-term (1982-2006) NDVI decline with correction of RF and AF effects and masking of saturated NDVI zone versus main land cover/use types is shown in Figure 11. The related statistics for countries and territories in the world are shown in Annex 2, and also summarized by major world regions in Table 2.

Table 2 shows at varying magnitudes of land degradation according to land use/cover types and geographic regions. One of the key highlights of this summary is the substantial shares of degradation in grasslands and shrublands, especially in North Africa and Near East (52%) and Sub-Saharan Africa (40%), which negatively affects the livelihoods of especially the pastoralist communities. In a related note, about 43% of the areas with sparse vegetation are degraded in Asia. Quite often, these areas also serve as grazing grounds for ruminants, for example in Central Asia (Pender et al. 2009). The share of cropland degradation seems especially high in Asia (30%), North Africa and Near East (45%), the regions with extensive irrigated agriculture. The absolute magnitudes of degrading areas are given in Annex 2.

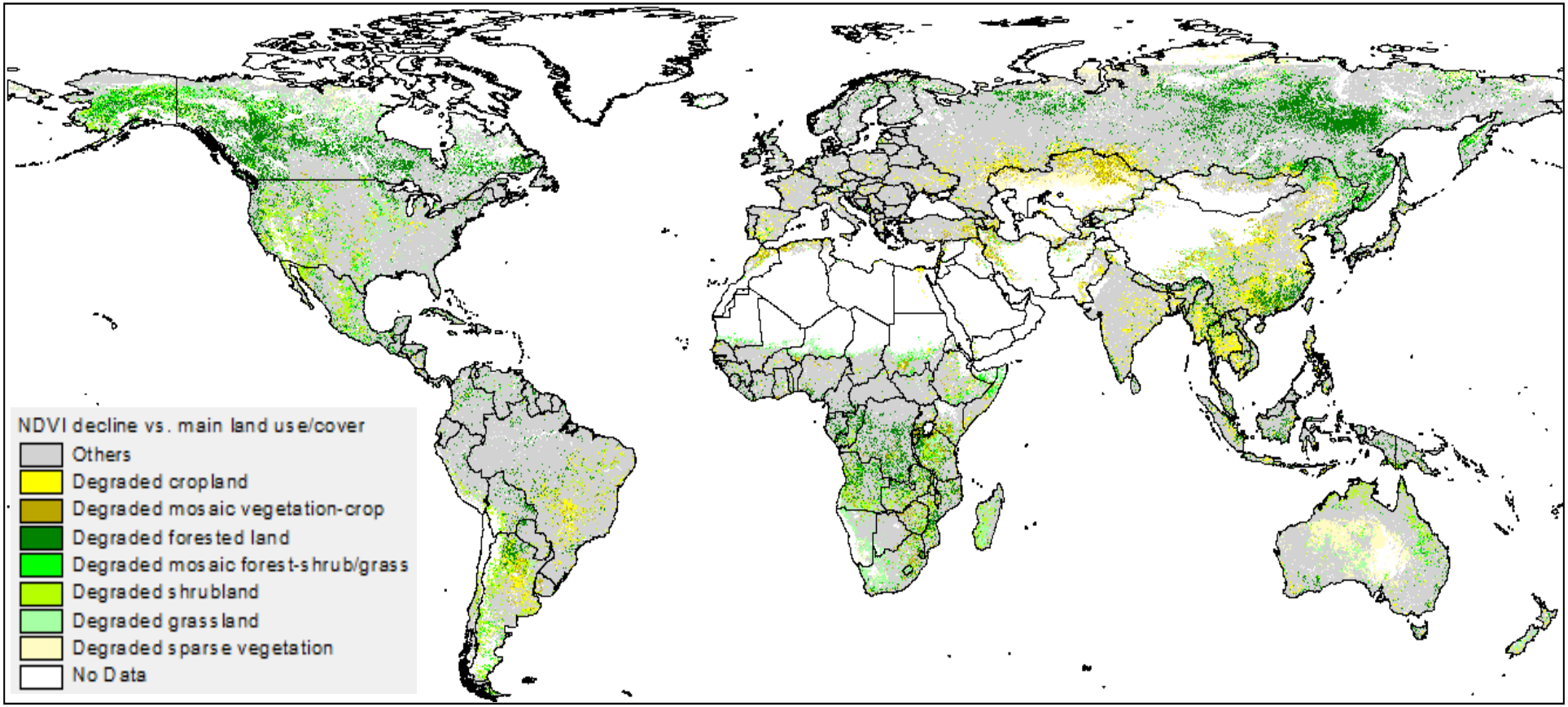

Figure 11. Areas of long-term (1982-2006) NDVI decline (with correction of RF and AF effects and masking saturated NDVI zone) versus main land cover/use types.

Table 2. The share of degrading area in each type of land cover by continental regions and world (unit: % of total area of a land cover type across a continental region).

Continents	Crop land	Mosaic vegetation- crop	Forested land	Mosaic forest- shrub/grass	Shrub land	Grass land	Sparse vegetation
Asia	30%	31%	30%	36%	33%	24%	43%
Europe	19%	21%	21%	20%	6%	17%	17%
North Africa and Near East	45%	42%	30%	36%	39%	52%	18%
Sub-Saharan Africa	12%	26%	26%	26%	28%	40%	29%
Latin America and Caribbean	25%	16%	10%	29%	29%	24%	34%
North America and Australasia	17%	16%	32%	36%	27%	40%	22%
World	**25%**	**25%**	**23%**	**29%**	**25%**	**33%**	**23%**

Note: the results in grey text should be treated with caution, see explanation in the next page.

These results in Figure 11, Table 2 and Annex 2 should be treated with special cautions regarding the following aspects:

- Although pixels of saturated greenness (LAI > 4) are masked out, the indication of biomass production dynamics using inter-annual NDVI trend in the forested areas (data in 2005-2006) may not be reliable compared to those of herbaceous vegetation types. The reason would be that most biomass of closed forest is in *the woody component whose annual dynamics (rather relatively slow or steady)* may not be necessary well-related to annual greenness of the forest canopy *(rather rapidly variable)*. Moreover, with forest ecosystems, especially those used for nature protection, biodiversity is often a prioritized task in the ecosystem assessments. However, increases of biomass production and/or soil nutrients may not necessarily be correlative with biodiversity maintenance. For example, invasion of exotic plant species can lead to high biomass productivity but dramatically reduce biodiversity, which is not desirable regarding the land-use purpose (Nkonya *et al.*, 2013). Increasing of soil nutrients can reduce plant diversity in some cases (Chapin *et al.*, 2000; Sala *et al.*, 2000; Wassen *et al.*, 2005).

- NDVI signal may not be a suitable indicator of degradation of sparse vegetation areas. When wet exposed soils tend to darken, i.e., soils' reflectance is a direct function of water content. If the spectral response to moistening is not exactly the same in the two spectral bands (IR and NIR), the NDVI of sparsely vegetative areas can appear to change as a result of soil moisture changes (precipitation or

evaporation) rather than because of vegetation changes[1]. Although soil-adjusted vegetation index (SAVIs) (Huete, 1988) can help improve the correlation between the index and the actual vegetation status, vegetation biomass itself may be not so crucial for indicating the status of the exposed soils.

- The attribution of "human-induced" degradation to the "rainfall- and atmospheric fertilization-corrected" NDVI decline makes sense in areas where there is no other natural drivers of biomass production decline besides the reduction of annual rainfall and atmospheric fertilization. Event-based wild fires which may be a factor that has likely reduced biomass production in remote, unpopulated regions like Alaska (Boles and Verbyla, 2000) or the inland of the Australian continent (Kasischke and Penner, 2004). Thus, the term "human-induced degradation" may be less applicable in these areas. Furthermore, the use of mean annual NDVI can reduce partly, but not eliminate completely the effects of change in the seasonality of weather parameters that are important in many climate change scenarios.

5.8 Potential soil degradation masked by fertilizer application

The trend of above ground biomass productivity can be an indirect indicator of soil degradation or soil improvement if the nutrient source for vegetation/crop growth is *solely*, or *largely*, from the soils (i.e., soil-based biomass productivity). In the agricultural areas with intensive application of mineral fertilizers (i.e., fertilizer-based crop productivity), the net primary productivity principally cannot be a reliable indicator of soil fertility trend (Le, 2012). In this case, alternative indicators of soil fertility should be used.

Global patterns of fertilizer applications, based on data reported in around 2000 (Potter *et al.*, 2010; MacDonald *et al.*, 2011), are shown in Figure 12. The amount of fertilizers used in East Asia (e.g. China and Vietnam), Northern India, Europe and in considerable areas in North America is equal to 18 - 20 times of those in sub-Saharan Africa (see Figure 12 and Table 3), which has been only around 1 kg/ha/year (Vlek *et al.*, 1997).

[1] http://en.wikipedia.org/wiki/Normalized_Difference_Vegetation_Index

a)

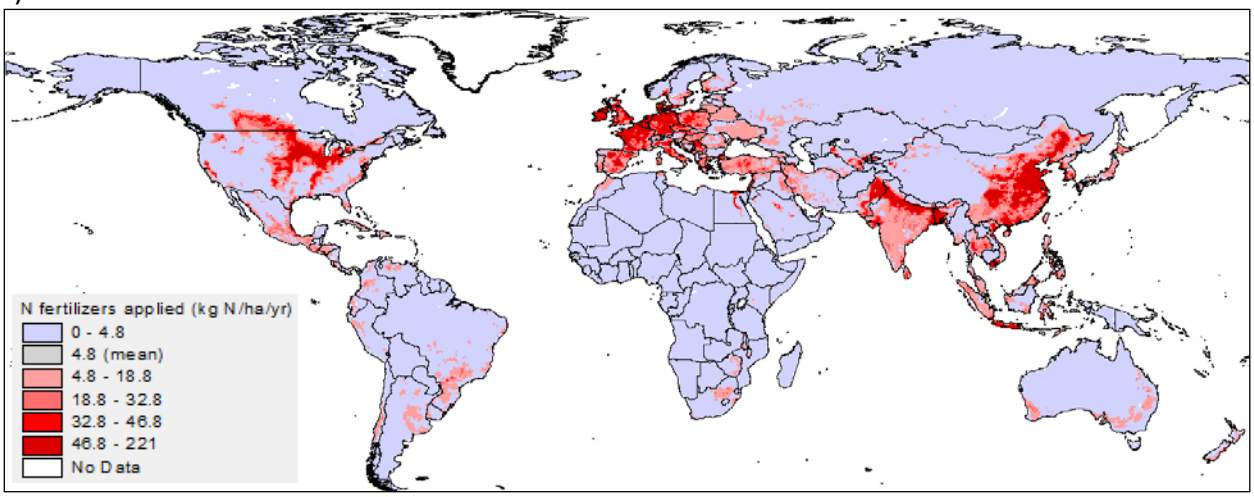

b)

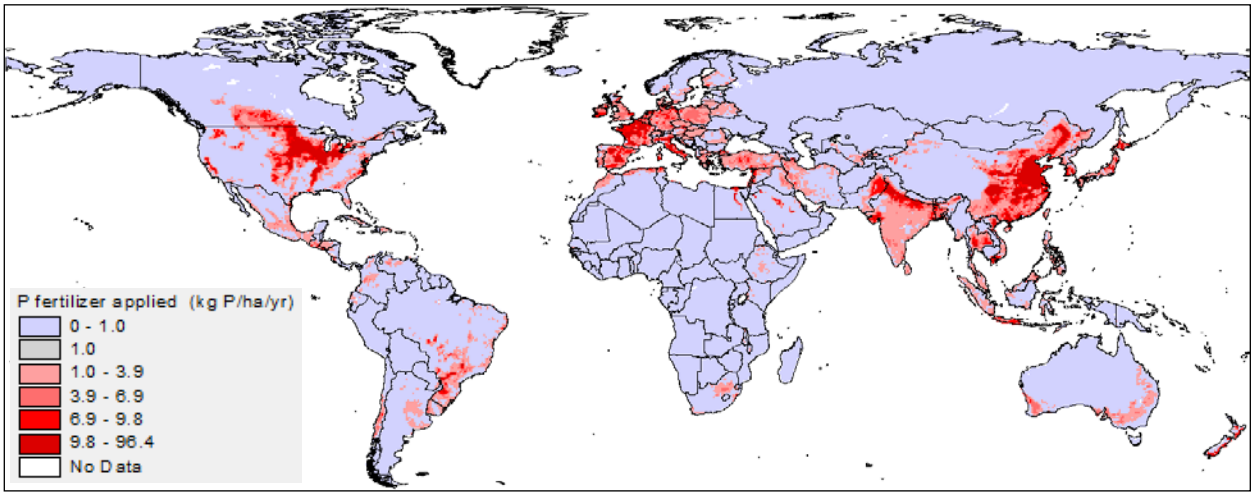

c)

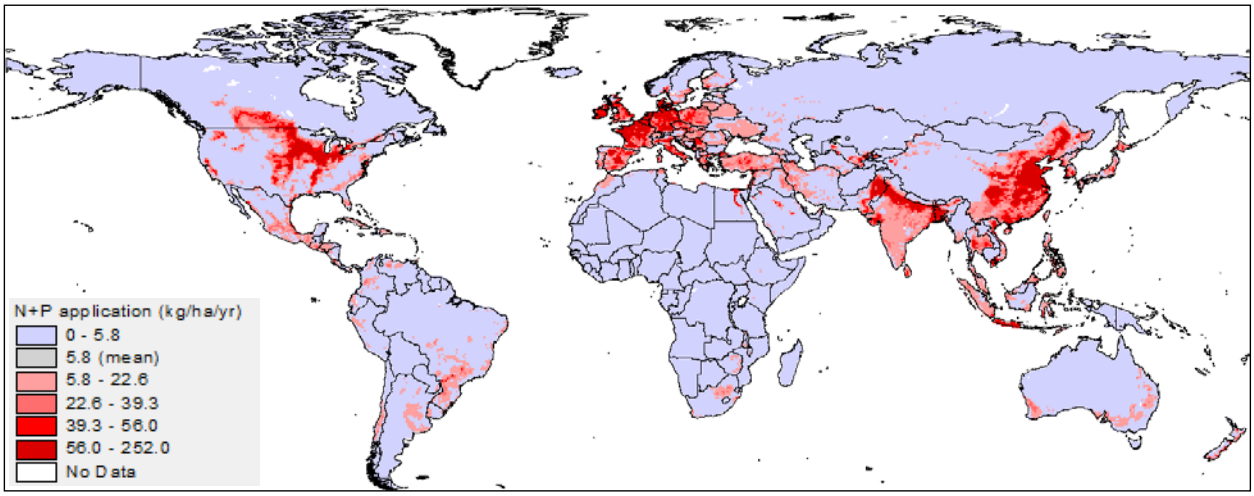

Figure 12. Global patterns of N and P fertilizers application for major crops in 2000. Data sources: (Potter *et al.*, 2010; MacDonald *et al.*, 2011). a) application of nitrogen fertilizer, b) application of phosphorus fertilizer, c) combination of nitrogen and phosphorus application.

Table 3. Fertilizer consumptions in different regions of the world in 2011 (in million metric tons)

Countries and Regions	Nitrogen	Phosphorous	Potash
China	33.8	11.5	5.2
India	17.4	8.0	2.6
United States	12.1	4.0	4.3
East Asia	41.7	14.1	9.5
South Asia	22.0	9.2	3.0
North America	14.4	4.8	4.6
Western and Central Europe	10.3	2.4	2.7
Latin America and the Caribbean	7.4	5.7	5.6
Eastern Europe and Central Asia	4.4	1.2	1.3
West Asia	2.9	1.1	0.3
Africa	3.3	1.0	0.5
Sub-Saharan Africa	1.7	0.6	0.4
World	**108**	**41**	**28**

Source: International Fertilizer Association (www.ifa.org, accessed on 06 February 2014). The figures for Sub-Saharan Africa were calculated by the authors' based on country fertilizer consumption statistics for Africa given by IFA.

Although the global spatial data of fertilizer use is available for year 2000 or around, the estimated regional averages and trends (Table 4) show that the 2000 fertilizer use maps can be used to depict the relative global patterns of the study period.

Table 4. Fertilizer uses (in million tons) and average annual growth rates (in %) in different periods

	Fertilizer Use			Annual Growth	
Regions	1959/60	1989/90	2020	1960-90	1990-2020
East Asia	1.2	31.4	55.7	10.9	1.9
South Asia	0.4	14.8	33.8	12	2.8
West Asia and North Africa	0.3	6.7	11.7	10.4	1.9
Latin America	0.7	8.2	16.2	8.2	2.3
Sub-Saharan Africa	0.1	1.2	4.2	5.5	1.2
World	**27.4**	**143.6**	**208**	**5.5**	**1.2**

Data source: FAO and the calculations by Bumb and Baanante (1996)

Pixels with remarkable fertilizer application (e.g. > 5.8 kg/ha/yr, i.e., the global mean) and neutral biomass productivity trend, may have a potential risk of soil degradation that cannot be detected by NDVI-based analysis. These areas are shown in Figure 13, accounting for about 7 million km^2, or 4.8% of global land area.

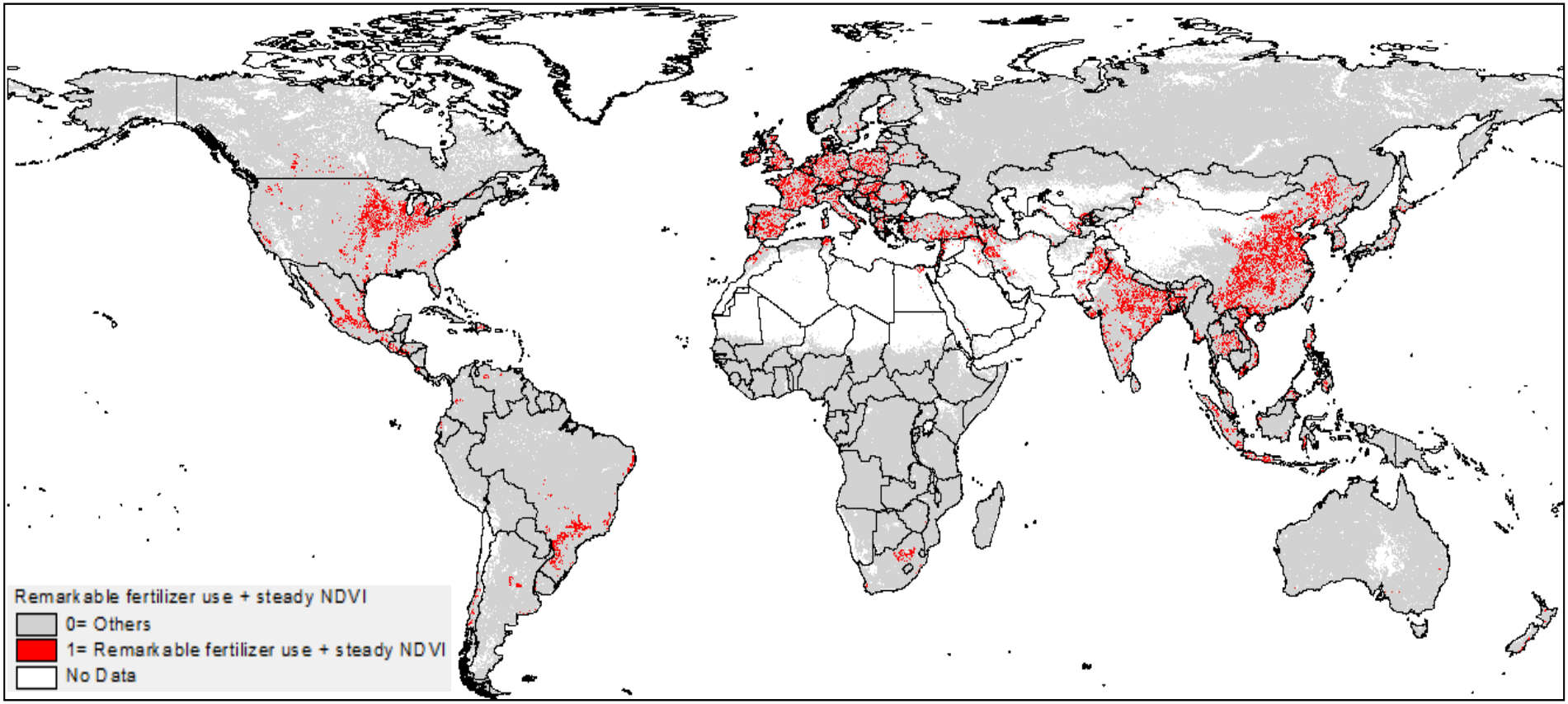

Figure 13. Pixels with remarkable fertilizer application (e.g. ≥ 12 kg N+P/ha/yr = twice of the global mean) but with neutral trend of biomass productivity, may have a potential risk of soil degradation

5.9 Areas of soil improvement

In addition to the areas with land degradation, we have also identified that there has been NDVI improvement in about 2.7% of global land area. The analysis identifies the areas of land improvement ("bright spots") by the increasing slope of inter-annual mean NDVIs: more by 10 % or more over 25 year and at 90% statistical significance. This is also adjusted/corrected for rainfall and atmospheric fertilization effects, LAI < 4), (Figure 14).

The major "bright spots" of land improvement are located in the Sahelian belt in Africa, Central parts of India, western and eastern coasts of Australia, central Turkey, areas of North-Eastern Siberia in Russia, and north-western parts of Alaska in the US.

Overlaying land degradation (Figures 10 and 13) with population density projections for 2010 (CIESIN-CIAT, 2005) shows that about 3.2 billion people are currently residing in degrading areas. Of this total number, about 0.6 billion people live in areas where land degradation is directly observed in the remotely sensed data, another 1.2 billion people live in areas where land degradation is likely masked by rainfall dynamics and atmospheric fertilization effects, finally, another 1.3 billion people reside in areas where chemical fertilization may be masking soil and land degradation. The regional breakdown of the population residing in degrading areas is given in Table 5 (The full data by country/territory is given in Annex 3). The biggest number of people residing in degrading areas is found in Asia, followed Europe, Middle East and North Africa, Latin America and Caribbean, Sub-Saharan Africa and finally, North America and Australasia. In terms of the share of people residing in degrading areas, the most affected are Middle East and North Africa, and Asia. In Asia and Europe, the higher shares of land degradation and of people residing in degrading areas are found in areas where land degradation might be masked by chemical fertilizer application. Whereas in other regions, visible decline and masking effects of rainfall and atmospheric fertilization seem to dominate. One caveat, these are still somewhat conservative estimates of the livelihoods which have potentially been affected by land degradation, because the number of people affected by land degradation is likely to be higher due to off-site and indirect externalities of land degradation.

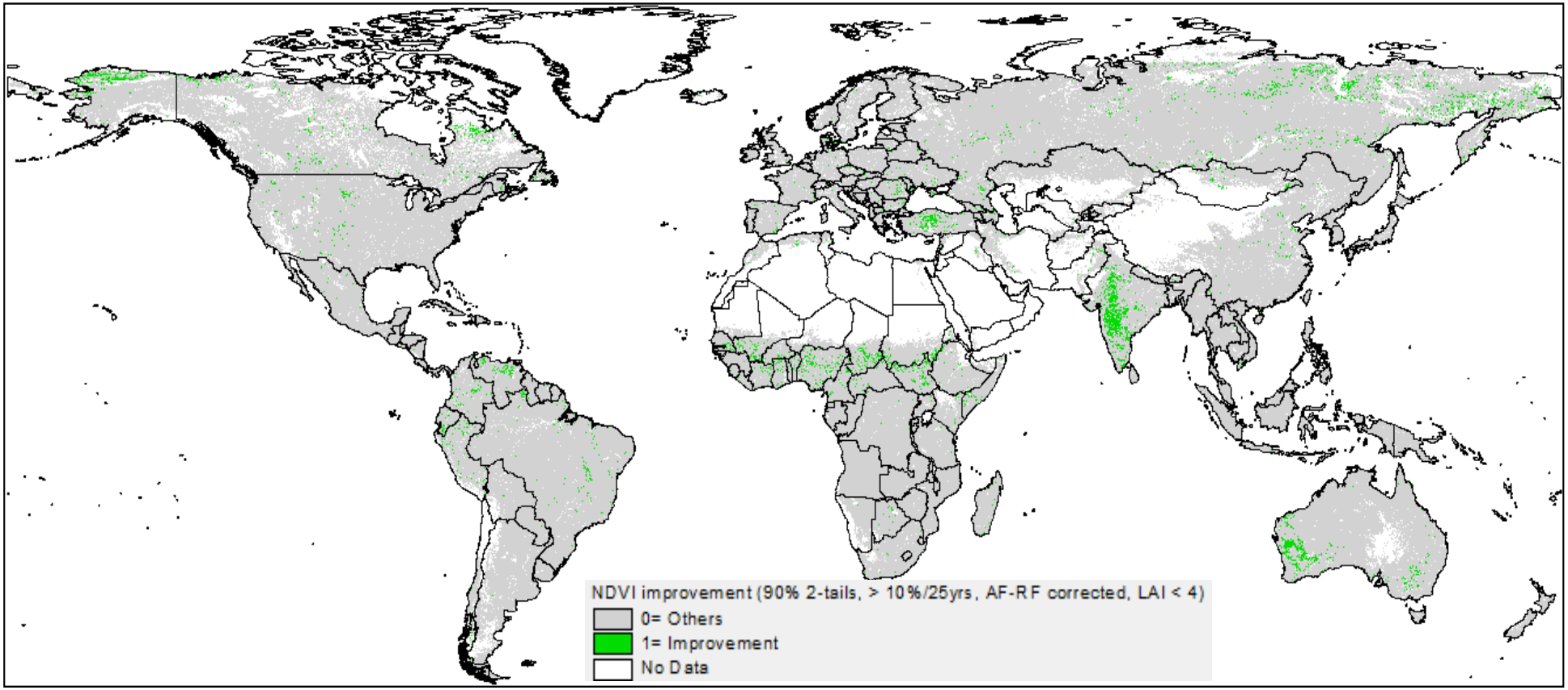

Figure 14. The areas of NDVI improvement, with slope of inter-annual mean NDVIs >= 10% over 25 year and 90% statistically significant, adjusted/corrected for RF and AF effects, LAI < 4.

Table 5. The number of people residing in degrading areas by region, the number in millions and the share in percentages

Regions	Visible degradation	Degradation masked by rainfall and atmospheric fertilization	Degradation masked by chemical fertilization	Total population in degrading areas	Total population in 2010	Share of population in degrading areas, %	Share of population in degrading areas, excluding areas with masking effect of chemical fertilization, %
Asia	434	834	1 055	2 324	4 184	56%	30%
Europe	11	48	143	203	575	35%	10%
Latin America and Caribbean	45	98	57	200	583	34%	25%
Middle East and North Africa	48	133	22	202	272	74%	66%
North America and Australasia	22	55	29	107	372	29%	21%
Sub-Saharan Africa	64	113	4	180	800	22%	22%
World	**624**	**1 282**	**1 310**	**3 216**	**6 787**	**47%**	**28%**

6. Conclusions

In this study, we advance the knowledge by making the following relatively new contributions. Firstly, the major contribution of this global study is the identification of regions *where* degradation magnitude and extent are *relatively high* for *prioritizing* both preventive investments for the restoration or reclamation of degraded land, and subsequent focal ground-based studies. The map of degradation hotspots is different from the production of an accurate map of all degraded areas that seems impractical at global level due to lacking data on many aspects of land degradation. Secondly, we account for masking effects of rainfall dynamics, atmospheric and anthropogenic fertilizations. To our knowledge, there has been no previous published study at global level accounting for all these masking factors. Moreover, we also identify the areas where land improvement has occurred.

The results show that land degradation hotspots stretch to about 29% of the total global land area and are occurring across all agro-ecologies. One third of this degradation is directly identifiable from a statistically significant declining trend in NDVI. However, the remaining two thirds of this degradation are concealed by rainfall dynamics, atmospheric fertilization and application of chemical fertilizers. Globally, human-induced biomass productivity decline are found in 25% of croplands and vegetation-crop mosaics, 29% of mosaics of forests with shrub- and grasslands, 25% of shrublands, and 33% of grasslands, as well as 23% of areas with sparse vegetation. The share of degrading croplands is likely to increase further when we take into account the croplands where intensive fertilizer application may be masking land degradation. Although this study does find land degradation to be a massive problem in croplands, it also emphasizes, in contrast to most previous similar studies, the extent of degradation in areas used for livestock grazing by pastoral communities, including grasslands, shrublands, their mosaics, and areas with sparse vegetation. In most countries, livestock production and its value chains produce comparable economic product and incomes for rural populations as crop production. In total, there are about 3.2 billion people who reside in these degrading areas. However, the true number of people affected by land degradation is likely to be higher, because even those people residing outside these degrading areas may be dependent on the continued flow of ecosystem goods and services from the degrading areas.

It is quite encouraging that about 2.7% of the global land mass has experienced significant improvement of biomass productivity over the last 25 years. However, the improving figure is modest as being 10 times smaller than the extent of areas with degrading lands, resulting extremely high net land degradation over the globe. Achieving the goal of Zero Net Land Degradation (Lal *et al.*, 2012) would, therefore, require considerable multiplication of efforts to rehabilitate degraded lands and also prevent further increasing rates of land degradation.

Despite being an advancement to the past studies on global land degradation mapping, the current work has several limitations. First, conceptually and practically the present study capture only the "primary productivity" aspect of land degradation. The other important aspects of land degradation such as soil/water pollution and biodiversity, which do not necessarily correlate with primary productivity, are still out of the scope of this study. Secondly, some degraded areas may not be captured by the NDVI-based assessment employed here, such as: the areas facing both human-induced and climate-driven declines, and areas facing biodiversity decline in natural vegetation. Thirdly, robustness of some key parametric procedures needs to be further evaluated. Moreover, the delineated degradation hotspots need to be validated by ground-level studies. This ground-level verification work is planned as the next step of our research activities. Further research is also required for evaluating the robustness and uncertainties of the presented results. The reported results (Figure 11, Table 2 and Figure 13) should be used as rough guides for geographic focus/prioritization in regional/national studies. The first activity of follow-up regional/national studies is to conduct activities for validating the “potential” hotspots. These may include the use of independent data, e.g., finer NDVI time-series like MODIS, accurate land cover change over the study period, soil degradation assessment (modeled erosion, leaching, change in key soil properties) (e.g., Le et al., 2012), change in species composition (e.g., Mbow et al. (2013)), fertilizer/water uses and yields.

The drivers of land degradation are numerous, complex and interrelated (Nkonya et al., 2011; Pender et al., 2009). In most cases, the effects of different land degradation drivers are modulated by context-specific factors (Nkonya *et al.*, 2013), necessitating local level in depth studies to identify the role of various factors on land degradation and improvement. The results

of global level correlative studies comparing several factors, such as population pressure, income per capita, poverty rates, governance (Vlek *et al.*, 2010; Nkonya *et al.*, 2011; Vu *et al.*, 2014) with land degradation provide with broadly useful estimates, but remain equivocal, due to difficulty of appropriately accounting for various omitted variables and endogeneity issues at such a broad scale. The results of this study are planned to be validated at the local level, and also would serve as a basis for the in-depth analysis of land degradation drivers through country case studies.

References

Bai, Z., Dent, D., Yu, Y., de Jong, R., 2013. Land degradation and ecosystem services. In: Lal, R., Lorenz, L., Hűttle, R.F., Schneider, B.U., Von Braun, J. (Eds.), Ecosystem Services and Carbon Sequestration in the Biosphere. Springer Dordrecht, pp. 357-381.

Bai, Z.G., Dent, D.L., Olsson, L., Schaepman, M.E., 2008a. Global Assessment of Land Degradation and Improvement 1. Identification by remote sensing. Report 2008/01. ISRIC - World Soil Information, Wageningen.

Bai, Z.G., Dent, D.L., Olsson, L., Schaepman, M.E., 2008b. Proxy global assessment of land degradation. Soil Use and Management 24, 223-234.

Bicheron, P., Defourny, P., Brockmann, C., Schouten, L., Vancutsem, C., Huc, M., Bontemps, S., Leroy, M., Achard, F., Herold, M., Ranera, F., Arino, O., 2008. GLOBCOVER: Products Description and Validation Report. http://due.esrin.esa.int/globcover/LandCover_V2.2/GLOBCOVER_Products_Description_Validation_Report_I2.1.pdf. ESA Globcover Project, led by MEDIAS-France/POSTEL.

Boisvenue, C., Running, S.W., 2006. Impacts of climate change on natural forest productivity - Evidence since the middle of the 20th century. Global Change Biology 12, 862 - 882.

Boles, S.H., Verbyla, D.B., 2000. Comparison of three AVHRR-based fire detection algorithms for interior Alaska. Remote Sens. Environ. 72, 1 –16.

Brown, M.E., Pinzon, J.E., Didan, K., Morisette, J.T., Tucker, C.J., 2006. Evaluation of the consistency of long-term NDVI time series derived from AVHRR, SPOT-Vegetation, SeaWIFS, MODIS and LandSAT ETM+. IEEE Transactions Geoscience and Remote Sensing 44, 1787-1793.

Buitenwerf, R., Bond, W.J., Stevens, N., Trollope, W.S.W., 2012. Increased tree densities in South African savannas: >50 years of data suggests CO2 as a driver. Global Change Biology 18, 675–684.

Bumb, B.L., Baanante, C.A., 1996. World Trends in Fertilizers Use and Projections to 2020. 2020 BRIEF - A 2020 Vision for Food, Agriculture, and the Environment 38 (October 1996), 1-2.

Carlson, T.N., Ripley, D.A., 1997. On the relation between NDVI, fractional vegetation cover, and leaf area index. Remote Sensing of Environment 62, 241-252.

Center for International Earth Science Information Network (CIESIN), Centro Internacional de Agricultura Tropical (CIAT), 2005. Gridded Population of the World Version 3 (GPWv3): Population Density Grids. http://sedac.ciesin.columbia.edu/gpw (accessed on 01 May 2013). Socio-economic Data and Applications Center (SEDAC), Columbia University, Palisades, NY.

Chapin, F.S.I., Zavaleta, E.S., Eviner, V.T., Naylor, R.L., Vitousek, P.M., Reynolds, H.L., Hooper, D.U., Lavorel, S., Sala, O.E., Hobbie, S.E., Mack, M.C., Diaz, S., 2000. Consequences of changing biodiversity. Nature 405, 234-242.

Conijn, J.G., Bai, Z.G., Bindraban, P.S., Rutgers, B., 2013. Global changes of net primary productivity, affected by climate and abrupt land use changes since 1981 — Towards mapping global soil degradation. Report 2013/01. ISRIC – World Soil Information, Wageningen.

de Jong, R., de Bruin, S., de Wit, A., Schaepman, M.E., Dent, D.L., 2011. Analysis of monotonic greening and browning trends from global NDVI time-series. Remote Sensing of Environment 115, 692-702.

de Jong, R., Verbesselt, J., Schaepman, M.E., de Bruin, S., 2012. Trend changes in global greening and browning: contribution of short-term trends to longer-term change. Global Change Biology 18, 642-655.

Dent, D., Bai, Z., Schaepman, M.E., Olsson, L., 2009. Letter to the Editor - Response to Wessels: Comments on 'Proxy global assessment of land degradation'. Soil Use and Management 25, 93 - 97.

Dentener, F.J., 2006. Global Maps of Atmospheric Nitrogen Deposition, 1860, 1993 and 2050 — Data Set. . Oak Ridge National Laboratory, Distributed Active Archive Center, Oak Ridge, Tennessee, U.S.A.

Diamond, J., 2005. Collapse: How societies choose to fail or succeed. Viking, New York, NY.

Dregne, H.E., 1977. Generalized Map of the Status of Desertification of Arid Lands. Report presented in the 1977 United Nations Conference on Desertification. FAO, UNESCO and WMO.

Dubovyk, O., Menz, G., Conrad, C., Kan, E., Machwitz, M., Khamzina, A., 2013. Spatio-temporal analyses of cropland degradation in the irrigated lowlands of Uzbekistan using remote-

sensing and logistic regression modeling. Environmental monitoring and assessment 185, 4775-4790.

Eswaran, H., Lal, R., Reich, P., 2001. Land Degradation: An Overview. In: E. Bridges, I. Hannam, L. Oldeman, F. Penning de Vries, S. Scherr, Sompatpanit, S. (Eds.), In Responses to Land Degradation. Proc. 2nd International Conference on Land Degradation and Desertification in Khon Kaen, Thailand. Oxford Press, New Delhi.

Evans, J., Geerken, R., 2004. Discrimination between climate and human-induced dryland degradation. Journal of Arid Environments 57, 535-554.

Fensholt, R., Langanke, T., Rasmussen, K., Reenberg, A., Prince, S.D., Tucker, C., Scholes, R.J., Le, Q.B., Bondeau, A., Eastman, R., Epstein, H., Gaughan, A.E., Hellden, U., Mbow, C., Olsson, L., Paruelo, J., Schweitzer, C., Seaquist, J., Wessels, K., 2012. Greenness in semi-arid areas across the globe 1981–2007 — an Earth Observing Satellite based analysis of trends and drivers. Remote Sensing of Environment 121, 144-158.

Fensholt, R., Rasmussen, K., Kaspersen, P., Huber, S., Horion, S., Swinnen, E., 2013. Assessing Land Degradation/Recovery in the African Sahel from Long-Term Earth Observation Based Primary Productivity and Precipitation Relationships. Remote Sensing 5, 664-686.

Fensholt, R., Rasmussen, K., Nielsen, T.T., Mbow, C., 2009. Evaluation of earth observation based long term vegetation trends: Intercomparing NDVI time series trend analysis consistency of Sahel from AVHRR GIMMS, Terra MODIS and SPOT VGT data. Remote Sensing of Environment 113, 1886 - 1898.

GLCF, accessed in 01 May 2013. Global Inventory Modeling and Mapping Studies (GIMMS) AVHRR 8km Normalized Difference Vegetation Index (NDVI), Bimonthly 1981-2006: Product Guide. http://glcf.umd.edu/library/guide/GIMMSdocumentation_NDVIg_GLCF.pdf. Global Land Cover Facility (GLCF), the University of Maryland.

Hellden, U., Tottrup, C., 2008. Regional desertification: A global synthesis. Global and Planetary Change 64, 169 - 176.

Herrmann, S., Assaf, A., Compton, J.T., 2005. Recent trends in vegetation dynamics in the African Sahel and their relationship to climate. Global Enviromental Change 15, 394-404.

Hill, J., Stellmes, M., Udelhoven, T., Roder, A., Sommer, S., 2008. Mediterranean desertification and land degradation: Mapping related land use change syndromes based on satellite observations. Global and Planetary Change 64, 146 - 157.

Huete, A.R., 1988. A soil-adjusted vegetation index (SAVI). Remote Sensing of Environment 25, 295-309.

Jones, P., Harris, I., 2008. CRU Time-Series (TS) High Resolution Gridded Datasets. http://badc.nerc.ac.uk/view/badc.nerc.ac.uk__ATOM__dataent_1256223773328276 (accessed on 01 May 2013). NCAS British Atmospheric Data Centre Climate Research Unit (CRU), University of East Anglia.

Kasischke, E.S., Penner, J.E., 2004. Improving global estimates of atmospheric emissions from biomass burning. J. Geophys. Res. 109, D14S01, .

Lal, R., Safriel, U., Boer, B., 2012. Zero Net Land Degradation: A New Sustainable Development Goal for Rio+ 20. Secretariat of the United Nations Convention to Combat Desertification (UNCCD), pp. 1-30. URL: http://www.unccd.int/Lists/SiteDocumentLibrary/secretariat/2012/Zero%2020Net%2020Land%2020Degradation%2020Report%2020UNCCD%2020May%202012%202020background.pdf (accessed 202020 August 202013).

Le, Q.B., 2012. Indicators of Global Soils and Land Degradation. Slides of Oral Presentation at the First Flobal Soil Week, 18-22 November 2012, Berlin, Germany. The First Global Soil Week, Berlin.

Le, Q.B., Tamene, L., Vlek, P.L.G., 2012. Multi-pronged assessment of land degradation in West Africa to assess the importance of atmospheric fertilization in masking the processes involved. Global and Planetary Change 92–93, 71-81.

Lewis, S.L., Lopez-Gonzalez, G., Sonké, B., Affum-Baffoe, K., Baker, T.R., 2009. Increasing carbon storage in intact African tropical forests. Nature 457, 1003-1006.

Liang, S., Xiao, Z., 2012. Global Land Surface Products: Leaf Area Index Product Data Collection (1985-2010). Beijing Normal University.

MacDonald, G.K., Bennett, E.M., Potter, P.A., Ramankutty, N., 2011. Agronomic phosphorus imbalances across the world's croplands. Proceedings of the National Academy of Sciences of the United States of America 108, 3086-3091.

Markon, C.J., Fleming, M.D., Binnian, E.F., 1995. Characteristics of vegetation phenology over the Alaskan landscape using AVHRR time-series data. Polar Record 31, 179-190.

Mbow, C., Fensholt, R., Rasmussen, K., Diop, D., 2013. Can vegetation productivity be derived from greenness in a semi-arid environment? Evidence from ground-based measurements. Journal of Arid Environments 97, 56-65.

MEA, 2005. Ecosystems and Human Well-being: Synthesis. Millennium Ecosystem Assessment. Washington DC.

Mitchell, T.D., Jones, P.D., 2005. An improved method for constructing a database of monthly climate observations and associated high-resolution grids. International Journal of Climatology 25, 693 - 712.

Nachtergaele, F., Petri, M., 2008. Mapping land use systems at global and regional scales for land degradation assessment analysis. FAO, Rome.

Nkonya, E., Braun, J.v., Mirzabaev, A., Le, Q.B., Kwon, H.Y., Kirui, O., 2013. Economics of Land Degradation Initiative: Methods and Approach for Global and National Assessments. ZEF - Discussion Papers on Development Policy 183, 1-41.

Nkonya, E., Gerber, N., Baumgartner, P., von Braun, J., De Pinto, A., Graw, V., Kato, E., Kloos, J., Walter, T., 2011. The Economics of Desertification, Land Degradation, and Drought - Toward an Integrated Global Assessment. ZEF-Discussion Papers on Development Policy No. 150, Center for Development Research (ZEF).

Oldeman, L.R., Hakkeling, R.T.A., Sombroek, W.G., 1990. World Map of The Status of Human-Induced Soil Degradation: An Explanatory Note (2nd ed.). International Soil Reference and Information Centre, Wageningen, the Netherlands.

Pettorelli, N., Vik, J.O., Mysterud, A., Gaillard, J.-M., Tucker, C.J., Stenseth, N.C., 2005. Using the satellite-derived NDVI to assess ecological responses to environmental change. Trends Ecol. Evol. 20, 503-510.

Pinter, P.J., Jackson, R.D., Elaine Ezra, C., Gausman, H.W., 1985. Sun-angle and canopy-architecture effects on the spectral reflectance of six wheat cultivars. International Journal of Remote Sensing 6, 1813-1825.

Pinzon, J., Brown, M.E., Tucker, C.J., 2005. Satellite time series correction of orbital drift artifacts using empirical mode decomposition. In: Huang, N.E., Shen, S.S.P. (Eds.), Hilbert-Huang Transform and Its Applications. World Scientific Publishing, Singapore, pp. 167-186.

Potter, P., Ramankutty, N., Bennett, E.M., Donner, S.D., 2010. Characterizing the Spatial Patterns of Global Fertilizer Application and Manure Production. Earth Interactions 14. Paper No. 2, 22 p. DOI:210.1175/2009ei1288.1171.

Reay, D.S., Dentener, F., Smith, P., Grace, J., Feely, R., 2008. Global nitrogen deposition and carbon sinks. Nature Geoscience 1, 430 - 437.

Safriel, U.N., 2007. The assessment of global trends in land degradation. In: Sivakumar, M.V.K., Ndiang'ui, N. (Eds.), Climate and Land Degradation. Springer Verlag, Berlin, pp. 1 - 38.

Sala, O.E., Chapin, F.S.I., Armesto, J.J., Berlow, E., Bloomfield, J., Dirzo, R., Huber-Sanwald, E., Huenneke, L.F., Jackson, R.B., Kinzig, A., Leemans, R., Lodge, D.M., Mooney, H.A., Oesterheld, M., Poff, N.L., Sykes, M.T., Walker, B.H., Walker, M., Wall, D., 2000. Global biodiversity scenarios for the year 2100. Science 287, 1770-1774.

Sommer, S., Zucca, C., Grainger, A., Cherlet, M., Zougmore, R., Sokona, Y., Hill, J., Della Peruta, R., Roehrig, J., Wang, G., 2011. Application of indicator systems for monitoring and assessment of desertification from national to global scales. Land Degradation & Development 22, 184-197.

Thomas, W., 1997. A three-dimensional model for calculating reflection functions of inhomogeneous and orographically structured natural landscapes. Remote Sensing of Environment 59, 44-63.

Trabucco, A., Zomer, R.J., 2009. Global Aridity Index (Global-Aridity) and Global Potential Evapo-Transpiration (Global-PET) Geospatial Database. CGIAR Consortium for Spatial Information, CGIAR-CSI GeoPortal: http://www.csi.cgiar.org.

Tucker, C.J., Pinzon, J.E., Brown, M.E., Slayback, D.A., Pak, E.W., Mahoney, R., Vremote, E.F., El Saleous, N., 2005. An extended AVHRR 8-km NDVI data set compatible with MODIS and SPOT Vegetation NDVI data. International Journal of Remote Sensing 26, 4485 - 4498.

UNCCD, 2004. UNCCD Ten Years On. Secretariat of the United Nations Convention to Combat Desertification (UNCCD), Bonn, Germany.

USDA-NRCS, 1998. Global Desertification Vulnerability Map. U.S. Department of Agriculture, Natural Resources Conservation Science (USDA-NRCS). URL: http://www.nrcs.usda.gov/wps/portal/nrcs/detail/national/nedc/training/soil/?cid=nrcs142p2_054003 (accessed on May 31th 2014).

Vlek, P., Le, Q.B., Tamene, L., 2010. Assessment of land degradation, its possible causes and threat to food security in Sub-Saharan Africa. In: Lal, R., Stewart, B.A. (Eds.), Food Security and Soil Quality. CRC Press, Boca Raton, Florida, pp. 57 - 86.

Vlek, P.L.G., Kühne, R.F., Denich, M., 1997. Nutrient resources for crop production in the tropics. Philos Trans R Soc Lond B Biol Sci 352, 975–985.

Vlek, P.L.G., Le, Q.B., Tamene, L., 2008. Land Decline in Land-Rich Africa: A Creeping Disaster in the Making. CGIAR Science Council Secretariat, Rome, Italy.

Vogt, J.V., Safriel, U., Maltitz, G.V., Sokona, Y., Zougmore, R., Bastin, G., Hill, J., 2011. Monitoring and assessment of land degradation and desertification: Towards new conceptual and integrated approaches. Land Degradation and Development 22, 150–165.

Vu, Q.M., Le, Q.B., Frossard, E., Vlek, P.L.G., 2014. Socio-economic and biophysical determinants of land degradation in Vietnam: An integrated causal analysis at the national level. Land Use Policy 36, 605-617.

Vu, Q.M., Le, Q.B., Vlek, P.L.G., 2013. Hotspots of human-induced biomass productivity decline and their social-ecological types towards support national policy and local studies on land degradation Global and Planetary Change, re-submitted in response to major revision requested November 2013.

Wassen, M.J., Olde Venterink, H., Lapshina, E.D., Tanneberger, F., 2005. Endangered plants persist under phosphorus limitation. Nature 437, 547-550.

Wessels, K.J., Prince, S.D., Malherbe, J., Small, J., Frost, P.E., VanZyl, D., 2007. Can human-induced land degradation be distinguished from the effects of rainfall variability? A case study in South Africa. Journal of Arid Environments 68, 271–297.

Xiao, Z., Liang, S., Wang, J., Chen, P., Yin, X., Zhang, L., Song, J., 2014. Use of General Regression Neural Networks for Generating the GLASS Leaf Area Index Product From Time-Series MODIS Surface Reflectance. Geoscience and Remote Sensing, IEEE Transactions on 52, 209-223.

Annex 1. Data sources used

Variable	*Used dataset /Resolution /Used period*	*Primary reference*
Annual mean NDVI	GIMMS NDVI 1982-2006, downloaded from the Global / 8 km/ 1982-2006 (biweekly)	(Tucker *et al.*, 2005)
Land cover type	GLOBCOVER version 2.2 / 300 m / average for 2004-2006	(Bicheron *et al.*, 2008)
Annual mean rainfall	CRU TS 3.1 / 0.5 deg /1982-2006 monthly	(Jones and Harris, 2008)
Aridity index-driven climate zone	CGIAR-CSI Global-Aridity data / 1 km / average for 1950-2000/	(Trabucco and Zomer, 2009)
Population density	CIESIN-CIAT Gridded Population of the World version 3 / 2.5 arc-minutes / 1990, 1995, 2000	(Center for International Earth Science Information Network (CIESIN) and Centro Internacional de Agricultura Tropical (CIAT), 2005)
Fertilizer (N and P) application	Global fertilizer (N and P) application / 0.5 deg / 2000	(Potter *et al.*, 2010)
Leaf Area Index	GLASS LAI / 8km /1982-2000 (8-day time-series)	(Liang and Xiao, 2012; Xiao *et al.*, 2014)

Annex 2. Long-term (1982-2006) NDVI decline (with correction of RF and AF effects and masking of saturated NDVI zone) by main land cover/use types for countries and territories.

Area of NDVI decline in km² and in percentages for the corresponding land cover

Country	Cropland	Mosaic vegetation-crop	Forested land	Mosaic forest-shrub/grass	Shrub land	Grassland	Sparse vegetation	*Total*
Afghanistan	18752 (35%)	32192 (32%)	1152 (51%)	128 (40%)	832 (14%)	55488 (27%)	1280 (4%)	109824 (17%)
Algeria	24128 (50%)	29376 (45%)	1024 (23%)	2432 (25%)	6784 (46%)	N/A	13824 (12%)	77568 (3%)
Azerbaijan	14272 (34%)	9408 (33%)	896 (8%)	1664 (32%)	3008 (28%)	0 (0%)	640 (8%)	29888 (36%)
Albania	1792 (11%)	192 (2%)	896 (9%)	N/A	896 (33%)	N/A	0 (0%)	3776 (14%)
Armenia	3648 (23%)	1792 (16%)	320 (6%)	64 (29%)	384 (16%)	0 (0%)	64 (17%)	6272 (22%)
Andorra	192 (50%)	N/A	0 (0%)	N/A	N/A	N/A	0 (0%)	192 (41%)
Angola	448 (58%)	47616 (50%)	226560 (36%)	25024 (48%)	177728 (57%)	86336 (60%)	6912 (53%)	570624 (46%)
Argentina	233536 (50%)	94592 (37%)	156800 (45%)	128000 (44%)	504448 (40%)	17152 (24%)	178944 (43%)	1313472 (48%)
Australia	69184 (9%)	1024 (7%)	161280 (19%)	99840 (21%)	374144 (23%)	231744 (28%)	1379712 (42%)	2316928 (30%)
Austria	6016 (19%)	N/A	10752 (17%)	512 (16%)	0 (0%)	1664 (52%)	1600 (12%)	20544 (25%)
Barbados	0 (0%)	0 (0%)	0 (0%)	N/A	N/A	N/A	N/A	0 (0%)
Botswana	N/A	13824 (13%)	960 (14%)	1792 (16%)	5248 (13%)	41792 (10%)	320 (23%)	63936 (11%)
Belgium	4032 (28%)	N/A	64 (1%)	64 (4%)	0 (0%)	2304 (40%)	256 (2%)	6720 (22%)
Bahamas	192 (18%)	192 (25%)	832 (36%)	320 (28%)	0 (0%)	320 (13%)	0 (0%)	1856 (19%)
Bangladesh	31488 (31%)	1920 (14%)	3328 (28%)	64 (100%)	4352 (41%)	1984 (52%)	N/A	43136 (33%)
Belize	128 (22%)	0 (0%)	2048 (11%)	64 (6%)	N/A	384 (43%)	N/A	2624 (12%)
Bosnia-Herzegovina	3968 (27%)	832 (7%)	1536 (5%)	448 (16%)	0 (0%)	1664 (38%)	0 (0%)	8448 (17%)
Bolivia	15552 (21%)	4608 (20%)	103744 (17%)	12416 (33%)	63360 (47%)	16512 (23%)	23040 (47%)	239232 (22%)
Myanmar	121408 (59%)	18304 (47%)	92608 (35%)	320 (33%)	76800 (42%)	2176 (56%)	N/A	311616 (48%)
Benin	320 (1%)	576 (9%)	1472 (5%)	64 (1%)	2304 (4%)	0 (0%)	N/A	4736 (4%)
Belarus	3776 (3%)	128 (0%)	1600 (1%)	0 (0%)	0 (0%)	192 (3%)	64 (5%)	5760 (3%)
Solomon Islands	640 (7%)	256 (7%)	1088 (10%)	0 (0%)	N/A	N/A	N/A	1984 (7%)
Brazil	355776 (21%)	113984 (11%)	254016 (6%)	7232 (8%)	223936 (17%)	8960 (7%)	192 (14%)	964096 (11%)
Bhutan	512 (26%)	384 (33%)	8768 (29%)	192 (37%)	320 (18%)	448 (18%)	0 (0%)	10624 (28%)
Bulgaria	2112 (4%)	0 (0%)	1024 (2%)	0 (0%)	384 (11%)	0 (0%)	512 (2%)	4032 (4%)
Brunei	256 (29%)	0 (0%)	192 (4%)	N/A	64 (100%)	N/A	N/A	512 (10%)
Burundi	128 (50%)	3840 (43%)	6656 (47%)	N/A	1600 (85%)	0 (0%)	N/A	12224 (48%)
Canada	8896 (9%)	14016 (7%)	2518720 (40%)	486528 (40%)	235520 (23%)	756544 (50%)	726016 (11%)	4746240 (52%)
Cambodia	41344 (55%)	4864 (27%)	14528 (28%)	0 (0%)	12608 (36%)	320 (100%)	N/A	73664 (42%)
Chad	5440 (5%)	3840 (5%)	3392 (6%)	5504 (8%)	4992 (4%)	41920 (33%)	2688 (13%)	67776 (5%)
Sri Lanka	832 (22%)	64 (11%)	8256 (16%)	N/A	256 (4%)	N/A	N/A	9408 (15%)
Congo	N/A	5888 (18%)	83904 (38%)	3200 (32%)	27520 (48%)	8128 (80%)	N/A	128640 (38%)
Zaire	640 (11%)	56960 (16%)	460352 (26%)	5504 (38%)	53120 (46%)	2560 (31%)	0 (0%)	579136 (26%)

Area of NDVI decline in km^2 and in percentages for the corresponding land cover

Country	Cropland	Mosaic vegetation-crop	Forested land	Mosaic forest-shrub/grass	Shrub land	Grassland	Sparse vegetation	*Total*
China	1077632 (40%)	412608 (30%)	691712 (45%)	97280 (39%)	172480 (39%)	368832 (26%)	102528 (24%)	2923072 (31%)
Chile	5504 (14%)	4480 (25%)	21824 (10%)	3264 (19%)	36224 (14%)	640 (2%)	6208 (7%)	78144 (11%)
Cameroon	1280 (5%)	896 (2%)	26560 (9%)	192 (1%)	1536 (2%)	128 (7%)	128 (25%)	30720 (6%)
Comoros	N/A	64 (25%)	128 (5%)	N/A	0 (0%)	N/A	N/A	192 (10%)
Colombia	8256 (9%)	4928 (6%)	74176 (10%)	4096 (7%)	3456 (27%)	19200 (20%)	64 (4%)	114176 (10%)
Costa Rica	1664 (21%)	1344 (8%)	4096 (16%)	0 (0%)	N/A	320 (20%)	N/A	7424 (15%)
Central African Rep	576 (5%)	128 (1%)	9728 (3%)	1024 (4%)	3648 (2%)	N/A	N/A	15104 (2%)
Cuba	2048 (17%)	3456 (17%)	8576 (25%)	2112 (13%)	N/A	15232 (55%)	0 (0%)	31424 (30%)
Cyprus	640 (30%)	N/A	512 (38%)	448 (44%)	704 (38%)	N/A	896 (27%)	3200 (35%)
Denmark	448 (1%)	N/A	0 (0%)	0 (0%)	0 (0%)	128 (2%)	0 (0%)	576 (1%)
Djibouti	N/A	N/A	N/A	0 (0%)	N/A	0 (0%)	0 (0%)	0 (0%)
Dominica	N/A	N/A	128 (25%)	N/A	0 (0%)	N/A	N/A	128 (17%)
Dominican Republic	640 (7%)	1216 (7%)	3264 (19%)	320 (28%)	N/A	320 (17%)	64 (100%)	5824 (12%)
Ecuador	960 (2%)	576 (5%)	3840 (3%)	64 (1%)	128 (1%)	1408 (9%)	64 (4%)	7040 (3%)
Egypt	20224 (61%)	448 (16%)	N/A	N/A	320 (27%)	0 (0%)	256 (5%)	21248 (2%)
Ireland	0 (0%)	N/A	128 (4%)	1088 (4%)	0 (0%)	9536 (13%)	0 (0%)	10752 (16%)
Equatorial Guinea	N/A	128 (6%)	4736 (20%)	0 (0%)	N/A	N/A	N/A	4864 (17%)
Estonia	1984 (14%)	N/A	448 (1%)	0 (0%)	0 (0%)	832 (15%)	64 (1%)	3328 (8%)
Eritrea	320 (7%)	448 (5%)	N/A	2304 (18%)	192 (25%)	1216 (6%)	3264 (12%)	7744 (8%)
El Salvador	128 (3%)	320 (4%)	1152 (29%)	0 (0%)	N/A	960 (25%)	N/A	2560 (12%)
Ethiopia	35904 (18%)	30976 (19%)	9984 (16%)	59776 (27%)	37824 (20%)	7808 (14%)	45888 (32%)	228160 (23%)
Czech Republic	6208 (12%)	N/A	1280 (3%)	64 (3%)	0 (0%)	1280 (30%)	384 (3%)	9216 (12%)
French Guiana	0 (0%)	N/A	2112 (3%)	N/A	64 (20%)	0 (0%)	N/A	2176 (2%)
Finland	0 (0%)	N/A	53056 (10%)	4608 (16%)	N/A	5184 (20%)	23616 (21%)	86464 (28%)
Faroe Islands	N/A	N/A	0 (0%)	0 (0%)	0 (0%)	256 (13%)	N/A	256 (18%)
France	49984 (15%)	N/A	4032 (2%)	192 (3%)	64 (1%)	7040 (26%)	2688 (1%)	64000 (12%)
Gambia, The	192 (5%)	128 (16%)	192 (10%)	0 (0%)	64 (4%)	N/A	N/A	576 (6%)
Gabon	N/A	2560 (18%)	59776 (27%)	128 (11%)	4032 (30%)	3776 (69%)	N/A	70272 (27%)
Georgia	5504 (20%)	1856 (15%)	1664 (4%)	448 (16%)	320 (8%)	3072 (52%)	256 (50%)	13120 (19%)
Ghana	384 (3%)	4928 (9%)	7424 (9%)	256 (2%)	7296 (11%)	64 (20%)	N/A	20352 (9%)
Grenada	0 (0%)	N/A	128 (50%)	N/A	N/A	N/A	N/A	128 (38%)
Greenland	N/A	N/A	N/A	0 (0%)	64 (0%)	320 (1%)	0 (0%)	384 (0%)
Germany	15680 (9%)	N/A	6592 (3%)	512 (5%)	192 (2%)	10752 (26%)	1856 (2%)	35584 (10%)
Guadeloupe	N/A	0 (0%)	256 (33%)	N/A	N/A	N/A	0 (0%)	256 (15%)
Greece	5312 (10%)	0 (0%)	1344 (3%)	128 (10%)	1152 (6%)	0 (0%)	1920 (4%)	9856 (8%)
Guatemala	576 (10%)	384 (6%)	15808 (23%)	3776 (25%)	N/A	5952 (46%)	N/A	26496 (25%)
Guinea	192 (2%)	2048 (6%)	16512 (14%)	384 (4%)	8192 (10%)	N/A	0 (0%)	27328 (11%)

Area of NDVI decline in km^2 and in percentages for the corresponding land cover

Country	Cropland	Mosaic vegetation-crop	Forested land	Mosaic forest-shrub/grass	Shrub land	Grassland	Sparse vegetation	*Total*
Guyana	320 (7%)	64 (4%)	16640 (9%)	384 (29%)	1024 (11%)	448 (23%)	N/A	18880 (10%)
Gaza Strip	64 (0%)	0 (0%)	N/A	N/A	N/A	N/A	192 (75%)	256 (71%)
Haiti	1728 (13%)	1216 (11%)	512 (33%)	0 (0%)	N/A	576 (56%)	64 (33%)	4096 (15%)
Honduras	2368 (16%)	2560 (11%)	16896 (28%)	832 (12%)	64 (100%)	2240 (41%)	N/A	24960 (22%)
Croatia	3456 (12%)	256 (2%)	320 (1%)	64 (3%)	0 (0%)	896 (30%)	0 (0%)	4992 (9%)
Hungary	12992 (15%)	N/A	832 (3%)	256 (9%)	N/A	128 (7%)	640 (4%)	14848 (16%)
Iceland	N/A	N/A	N/A	1408 (3%)	0 (0%)	11968 (31%)	2368 (3%)	15744 (16%)
Indonesia	129984 (18%)	8320 (9%)	220992 (23%)	64 (0%)	13952 (35%)	64 (100%)	N/A	373376 (21%)
India	289024 (13%)	25344 (11%)	115392 (31%)	448 (22%)	25344 (19%)	17664 (11%)	0 (0%)	473216 (16%)
Iran	52928 (45%)	76224 (55%)	576 (2%)	24832 (46%)	8192 (39%)	1152 (4%)	83392 (29%)	247296 (15%)
Israel	3200 (76%)	2624 (63%)	0 (0%)	64 (33%)	256 (100%)	N/A	256 (20%)	6400 (30%)
Italy	25088 (14%)	N/A	3712 (3%)	128 (11%)	1216 (10%)	704 (37%)	3328 (5%)	34176 (12%)
Ivory Coast	704 (7%)	5568 (6%)	17088 (12%)	512 (6%)	7936 (14%)	0 (0%)	N/A	31808 (10%)
Iraq	9728 (39%)	11520 (37%)	128 (40%)	3072 (24%)	960 (36%)	N/A	17088 (21%)	42496 (10%)
Japan	49472 (41%)	320 (10%)	36800 (12%)	384 (23%)	384 (12%)	1728 (54%)	64 (10%)	89152 (24%)
Jamaica	192 (12%)	384 (13%)	1664 (28%)	0 (0%)	N/A	0 (0%)	N/A	2240 (21%)
Jordan	2240 (83%)	1152 (86%)	N/A	0 (0%)	N/A	N/A	2048 (24%)	5504 (6%)
Kenya	15808 (31%)	40512 (42%)	21568 (46%)	9664 (10%)	21952 (42%)	15232 (18%)	2688 (4%)	127424 (22%)
Kyrgyzstan	8192 (21%)	4736 (18%)	768 (13%)	384 (10%)	N/A	22784 (38%)	3072 (11%)	39936 (21%)
North Korea	1024 (55%)	N/A	32896 (39%)	11008 (37%)	320 (4%)	640 (77%)	8448 (40%)	54336 (45%)
South Korea	4544 (41%)	N/A	15616 (23%)	5888 (27%)	448 (6%)	192 (50%)	2944 (40%)	29632 (31%)
Kazakhstan	341696 (57%)	377920 (67%)	9088 (21%)	5760 (34%)	0 (0%)	38016 (38%)	847104 (66%)	1619584 (60%)
Laos	15104 (55%)	4736 (25%)	26048 (25%)	64 (14%)	28480 (33%)	128 (100%)	N/A	74560 (32%)
Lebanon	1728 (37%)	960 (22%)	0 (0%)	0 (0%)	128 (37%)	N/A	960 (52%)	3776 (37%)
Latvia	3328 (15%)	N/A	3328 (5%)	0 (4%)	0 (0%)	512 (11%)	192 (2%)	7360 (12%)
Lithuania	3200 (7%)	N/A	512 (1%)	64 (0%)	0 (0%)	1600 (28%)	128 (1%)	5504 (9%)
Liberia	N/A	2304 (7%)	11968 (20%)	0 (0%)	0 (0%)	N/A	N/A	14272 (15%)
Slovakia	3136 (14%)	N/A	704 (3%)	0 (0%)	0 (0%)	384 (18%)	448 (5%)	4672 (10%)
Liechtenstein	0 (0%)	N/A	64 (0%)	N/A	N/A	N/A	N/A	64 (40%)
Lesotho	N/A	2496 (33%)	1856 (42%)	2304 (42%)	2624 (64%)	7296 (55%)	N/A	16576 (55%)
Luxembourg	0 (0%)	N/A	0 (0%)	0 (0%)	N/A	0 (0%)	0 (0%)	0 (0%)
Libya	896 (39%)	3008 (70%)	N/A	448 (21%)	2112 (63%)	N/A	3776 (31%)	10240 (1%)
Madagascar	N/A	2560 (4%)	18304 (15%)	7936 (51%)	87744 (40%)	131776 (73%)	N/A	248320 (43%)
Martinique	0 (0%)	0 (0%)	448 (50%)	N/A	N/A	N/A	N/A	448 (42%)
Moldova	1984 (7%)	64 (1%)	0 (0%)	0 (0%)	0 (0%)	0 (0%)	0 (0%)	2048 (6%)
Mayotte	N/A	0 (0%)	0 (0%)	N/A	N/A	N/A	N/A	0 (0%)
Mongolia	45312 (23%)	49984 (16%)	11456 (18%)	1728 (16%)	704 (29%)	15296 (17%)	29120 (8%)	153600 (10%)

Area of NDVI decline in km^2 and in percentages for the corresponding land cover

Country	Cropland	Mosaic vegetation-crop	Forested land	Mosaic forest-shrub/grass	Shrub land	Grassland	Sparse vegetation	*Total*
Malawi	576 (50%)	6720 (31%)	11072 (34%)	1088 (57%)	17984 (51%)	1472 (56%)	N/A	38912 (41%)
Macedonia	704 (8%)	320 (4%)	256 (2%)	0 (0%)	128 (7%)	0 (0%)	N/A	1408 (6%)
Mali	5824 (5%)	9152 (12%)	192 (2%)	8832 (19%)	3648 (4%)	48192 (34%)	7872 (22%)	83712 (7%)
Morocco	42368 (53%)	26496 (53%)	640 (48%)	6336 (38%)	8576 (55%)	N/A	15296 (19%)	99712 (22%)
Mauritius	N/A	0 (0%)	192 (27%)	N/A	0 (0%)	N/A	N/A	192 (9%)
Mauritania	768 (13%)	7872 (39%)	N/A	11648 (46%)	0 (0%)	56960 (52%)	8832 (32%)	86080 (8%)
Oman	0 (0%)	0 (0%)	0 (0%)	N/A	0 (0%)	N/A	128 (4%)	128 (0%)
Montenegro	2240 (49%)	768 (19%)	832 (15%)	128 (18%)	64 (7%)	1472 (74%)	N/A	5504 (41%)
Mexico	25472 (34%)	61120 (31%)	112448 (22%)	91328 (36%)	314752 (37%)	82560 (40%)	0 (0%)	687680 (35%)
Malaysia	17280 (15%)	704 (6%)	32000 (17%)	N/A	704 (15%)	N/A	N/A	50688 (15%)
Mozambique	2048 (24%)	41920 (33%)	151872 (32%)	4544 (59%)	79040 (47%)	3968 (51%)	N/A	283392 (36%)
New Caledonia	384 (6%)	0 (0%)	2240 (23%)	0 (0%)	384 (20%)	N/A	N/A	3008 (16%)
Niger	3328 (21%)	12800 (49%)	64 (100%)	8000 (49%)	0 (0%)	138176 (55%)	4992 (17%)	167360 (13%)
Vanuatu	192 (5%)	64 (3%)	448 (9%)	N/A	N/A	N/A	N/A	704 (6%)
Nigeria	12160 (4%)	14784 (10%)	20736 (11%)	1728 (7%)	9984 (5%)	9216 (18%)	640 (21%)	69248 (8%)
Netherlands	2688 (18%)	N/A	128 (2%)	128 (4%)	0 (0%)	3008 (23%)	256 (3%)	6208 (18%)
Norway	0 (0%)	N/A	32256 (14%)	4608 (17%)	N/A	3392 (17%)	59776 (17%)	100032 (33%)
Nepal	16064 (30%)	3072 (15%)	8576 (19%)	768 (29%)	3264 (30%)	2944 (17%)	N/A	34688 (24%)
Suriname	0 (0%)	0 (0%)	2304 (2%)	0 (0%)	0 (0%)	192 (12%)	N/A	2496 (2%)
Nicaragua	4608 (17%)	2560 (8%)	9280 (17%)	320 (14%)	64 (20%)	1792 (35%)	0 (0%)	18624 (15%)
New Zealand	32832 (28%)	256 (3%)	9088 (11%)	2176 (10%)	4096 (9%)	38080 (66%)	N/A	86528 (33%)
Paraguay	8448 (12%)	3776 (10%)	29056 (13%)	0 (0%)	9664 (14%)	1536 (8%)	0 (0%)	52480 (13%)
Peru	8512 (17%)	1472 (13%)	30080 (4%)	2240 (10%)	41600 (20%)	16512 (27%)	5312 (9%)	105728 (8%)
Pakistan	57472 (21%)	11008 (15%)	2176 (33%)	128 (20%)	1984 (6%)	13376 (10%)	1152 (7%)	87296 (11%)
Poland	36672 (16%)	N/A	2816 (2%)	128 (3%)	0 (0%)	1152 (12%)	2624 (3%)	43392 (14%)
Panama	512 (5%)	64 (1%)	3712 (8%)	0 (0%)	64 (4%)	704 (30%)	N/A	5056 (7%)
Portugal	8768 (28%)	0 (0%)	320 (2%)	384 (12%)	6208 (23%)	0 (0%)	4480 (15%)	20160 (22%)
Papua New Guinea	16576 (12%)	2368 (9%)	55488 (21%)	64 (14%)	5248 (53%)	N/A	N/A	79744 (18%)
Pacific Islands (Palau)	128 (67%)	N/A	0 (0%)	N/A	N/A	N/A	N/A	128 (28%)
Guinea-Bissau	64 (7%)	384 (4%)	2368 (14%)	0 (0%)	1024 (20%)	N/A	N/A	3840 (14%)
Reunion	N/A	128 (12%)	384 (30%)	N/A	0 (0%)	0 (0%)	N/A	512 (20%)
Romania	6912 (5%)	0 (0%)	1664 (2%)	64 (1%)	0 (0%)	960 (8%)	384 (1%)	9984 (4%)
Philippines	39040 (22%)	1664 (14%)	19200 (24%)	64 (3%)	2048 (29%)	N/A	N/A	62016 (21%)
Puerto Rico	0 (0%)	0 (0%)	256 (5%)	0 (0%)	N/A	64 (20%)	N/A	320 (4%)
Russia	562048 (27%)	183296 (27%)	4074176 (24%)	482944 (22%)	116416 (6%)	162176 (17%)	1401792 (19%)	6982848 (43%)
Rwanda	960 (88%)	9216 (80%)	5504 (62%)	0 (0%)	1728 (93%)	128 (100%)	N/A	17536 (71%)
Saudi Arabia	448 (7%)	0 (0%)	0 (0%)	N/A	512 (14%)	N/A	1920 (8%)	2880 (0%)

Area of NDVI decline in km^2 and in percentages for the corresponding land cover

Country	Cropland	Mosaic vegetation-crop	Forested land	Mosaic forest-shrub/grass	Shrub land	Grassland	Sparse vegetation	*Total*
South Africa	2944 (26%)	97088 (39%)	68992 (35%)	28672 (39%)	47552 (42%)	251328 (43%)	47552 (46%)	544128 (45%)
Senegal	9280 (13%)	9216 (20%)	1920 (8%)	1088 (12%)	1344 (3%)	2112 (20%)	1408 (36%)	26368 (14%)
Slovenia	640 (16%)	N/A	640 (3%)	0 (0%)	0 (0%)	384 (30%)	0 (0%)	1664 (8%)
Sierra Leone	0 (0%)	3328 (8%)	6144 (19%)	0 (0%)	128 (4%)	N/A	N/A	9600 (13%)
San Marino	0 (0%)	N/A	N/A	N/A	N/A	N/A	N/A	64 (100%)
Singapore	128 (17%)	N/A	N/A	N/A	N/A	N/A	N/A	128 (18%)
Somalia	22912 (30%)	22016 (28%)	2752 (32%)	58304 (46%)	11072 (22%)	85952 (60%)	32832 (41%)	235840 (38%)
Spain	61632 (29%)	64 (5%)	5376 (4%)	5824 (24%)	20608 (23%)	0 (0%)	34560 (20%)	128064 (26%)
Serbia	3904 (7%)	128 (1%)	128 (0%)	64 (3%)	0 (0%)	64 (6%)	N/A	4288 (5%)
St. Lucia	0 (0%)	N/A	64 (17%)	0 (0%)	N/A	N/A	N/A	64 (10%)
Sudan	26624 (17%)	41472 (26%)	5696 (4%)	49664 (16%)	17344 (6%)	108608 (43%)	25408 (23%)	274816 (12%)
Svalbard	N/A	N/A	N/A	0 (0%)	0 (0%)	0 (0%)	256 (1%)	256 (0%)
Sweden	256 (3%)	N/A	75648 (12%)	2496 (9%)	0 (0%)	5184 (20%)	24576 (16%)	108160 (26%)
Syria	9408 (30%)	4160 (24%)	0 (0%)	2048 (38%)	1152 (33%)	N/A	6592 (17%)	23360 (13%)
Switzerland	1856 (17%)	N/A	1472 (6%)	128 (5%)	64 (2%)	1536 (38%)	0 (0%)	5056 (13%)
Trinidad and Tobago	0 (0%)	64 (9%)	192 (5%)	N/A	N/A	0 (0%)	N/A	256 (5%)
Thailand	212096 (65%)	15808 (48%)	39424 (46%)	0 (0%)	36160 (56%)	4736 (82%)	N/A	308224 (60%)
Tajikistan	7360 (23%)	1344 (16%)	0 (0%)	0 (0%)	0 (0%)	8704 (15%)	64 (3%)	17472 (12%)
Togo	192 (4%)	768 (15%)	1216 (8%)	64 (2%)	3392 (12%)	N/A	N/A	5632 (10%)
Sao Tome and Principe	N/A	0 (0%)	64 (9%)	N/A	N/A	N/A	N/A	64 (7%)
Tunisia	7040 (30%)	2560 (19%)	384 (35%)	576 (22%)	256 (33%)	N/A	6016 (17%)	16832 (11%)
Turkey	42752 (16%)	43584 (13%)	5376 (4%)	5120 (14%)	16192 (13%)	N/A	7616 (13%)	120640 (16%)
Taiwan	1728 (15%)	0 (0%)	4928 (23%)	N/A	1024 (34%)	N/A	N/A	7680 (24%)
Turkmenistan	22592 (32%)	10624 (27%)	N/A	0 (0%)	0 (0%)	2304 (23%)	1216 (10%)	36736 (8%)
Tanzania	12608 (32%)	112768 (62%)	139968 (36%)	18688 (76%)	93504 (70%)	75712 (76%)	640 (30%)	453888 (51%)
Uganda	8576 (20%)	15616 (24%)	9984 (30%)	1792 (12%)	6592 (14%)	0 (0%)	0 (0%)	42560 (21%)
United Kingdom	3712 (5%)	N/A	640 (3%)	5568 (4%)	0 (0%)	18880 (13%)	192 (1%)	28992 (12%)
Ukraine	70592 (13%)	8128 (6%)	3776 (3%)	768 (4%)	0 (0%)	896 (14%)	2112 (9%)	86272 (15%)
United States	173120 (25%)	207424 (18%)	912448 (23%)	609920 (37%)	840896 (32%)	707584 (37%)	236672 (30%)	3688064 (40%)
Burkina Faso	7104 (6%)	4544 (7%)	128 (5%)	2176 (11%)	2496 (6%)	3200 (19%)	1216 (13%)	20864 (8%)
Uruguay	6720 (19%)	17920 (15%)	1536 (23%)	0 (0%)	11200 (30%)	128 (4%)	N/A	37504 (21%)
Uzbekistan	25728 (26%)	960 (11%)	N/A	N/A	0 (0%)	4032 (17%)	4416 (16%)	35136 (8%)
Venezuela	2880 (5%)	4608 (4%)	40256 (8%)	2240 (4%)	2368 (23%)	23744 (20%)	128 (5%)	76224 (9%)
Vietnam	38720 (33%)	11200 (18%)	19456 (26%)	192 (50%)	19520 (28%)	960 (26%)	0 (0%)	90048 (29%)
Namibia	N/A	14080 (30%)	1088 (45%)	5952 (40%)	5504 (40%)	178496 (33%)	44928 (31%)	250048 (30%)
West Bank	2304 (93%)	1280 (95%)	N/A	N/A	N/A	N/A	512 (32%)	4096 (73%)
Swaziland	256 (67%)	2304 (61%)	6208 (63%)	448 (53%)	1792 (61%)	64 (20%)	N/A	11072 (64%)

Area of NDVI decline in km^2 and in percentages for the corresponding land cover

Country	Cropland	Mosaic vegetation-crop	Forested land	Mosaic forest-shrub/grass	Shrub land	Grassland	Sparse vegetation	*Total*
Yemen	2496 (21%)	128 (13%)	128 (29%)	64 (17%)	2240 (16%)	320 (38%)	3008 (13%)	8384 (2%)
Zambia	64 (33%)	35648 (43%)	136576 (42%)	18176 (48%)	115904 (50%)	29632 (45%)	64 (33%)	336064 (45%)
Zimbabwe	640 (100%)	70144 (52%)	24128 (57%)	10560 (53%)	58048 (50%)	39872 (46%)	0 (0%)	203392 (53%)

Note: (1) Land cover data extracted from Globcover data in 2005-2006 with the original resolution at 300 m, (2) results in grey text should be treated with special cautions (refer to section 4.9 for explanations), (3) The total area in the table is retrieved from the World Bank Development indicators for 2010/2012, (4) This listing of countries and territories does not necessarily reflect the opinion or official position of the authors, their affiliated institutions and of the funding agency on their legal status and are presented here in purely geographic sense.

Annex 3. The population residing in the areas with long-term (1982-2006) NDVI decline, including the areas with correction of RF and AF effects, and potential masking by chemical fertilization.

Country/Territory	Population residing in the areas with NDVI decline		Including the share in the areas with,		
	Total	Share of total	NDVI decline detected from the remotely sensed data	NDVI decline likely masked by CO_2 effects	NDVI decline likely masked by chemical fertilization
Afghanistan	16 852 408	53.7	13%	41%	0%
Albania	290 448	8.7	1%	7%	0%
Algeria	15 106 155	42.4	15%	27%	0%
Angola	4 037 106	22.7	10%	13%	0%
Argentina	18 802 484	45.3	16%	27%	2%
Armenia	1 884 852	49.8	7%	32%	11%
Australia	1 748 056	8.4	3%	4%	2%
Austria	2 383 705	29.9	2%	6%	22%
Azerbaijan	4 041 966	47.7	15%	30%	3%
Bangladesh	136 758 832	81.8	17%	20%	44%
Belarus	1 447 586	14.8	0%	2%	13%
Belgium	6 189 343	59.9	1%	15%	43%
Benin	516 278	6.2	2%	5%	0%
Bhutan	240 035	8.7	3%	4%	1%
Bolivia	2 942 555	28.8	9%	20%	0%
Bosnia-Herzegovina	644 980	15.2	2%	9%	4%
Botswana	251 710	15.5	8%	7%	0%
Brazil	61 522 576	32.2	6%	16%	10%
Brunei Darussalam	4 857	1.3	0%	1%	0%
Bulgaria	280 779	3.9	1%	2%	1%
Burkina Faso	2 308 837	14.7	3%	12%	0%
Burundi	2 035 828	23.6	16%	7%	0%
Cambodia	9 869 171	59.2	16%	40%	2%
Cameroon	249 638	1.4	0%	1%	0%
Canada	9 328 043	28.0	5%	12%	11%
Central African Republic	8 973	0.2	0%	0%	0%
Chad	1 065 378	10.0	2%	8%	0%
Chile	7 856 254	46.3	18%	22%	6%
China	913 036 224	68.0	13%	24%	31%
Colombia	8 522 501	17.4	6%	8%	3%
Congo	1 238 547	29.3	11%	18%	0%
Congo, Democratic Republic	10 598 746	14.9	3%	12%	0%
Costa Rica	551 072	11.3	1%	3%	8%
Croatia	1 012 785	22.7	0%	6%	17%
Cuba	2 762 277	24.0	4%	20%	0%
Czech Republic	2 729 091	26.9	3%	5%	19%
Denmark	885 588	16.5	0%	1%	15%
Djibouti	432 793	63.8	4%	60%	0%
Dominican Republic	2 572 894	26.7	1%	6%	20%
East Timor	201 452	30.1	2%	28%	0%
Ecuador	1 343 570	9.0	0%	7%	1%
Egypt	72 750 080	91.7	12%	70%	10%
El Salvador	4 723 999	63.7	0%	11%	52%
Equatorial Guinea	3 344	0.6	0%	0%	0%
Eritrea	1 371 472	26.9	7%	20%	0%
Estonia	181 745	14.5	0%	14%	0%

Country/Territory	Population residing in the areas with NDVI decline		Including the share in the areas with,		
	Total	Share of total	NDVI decline detected from the remotely sensed data	NDVI decline likely masked by CO_2 effects	NDVI decline likely masked by chemical fertilization
Ethiopia	16 958 654	21.2	7%	14%	0%
Finland	398 249	7.7	1%	0%	7%
France	27 162 878	44.4	1%	9%	34%
Gabon	23 422	1.5	0%	1%	0%
Gambia	436 293	27.2	2%	26%	0%
Georgia	665 321	13.4	6%	7%	1%
Germany	30 649 678	37.7	0%	5%	32%
Ghana	3 547 032	14.8	7%	8%	0%
Greece	2 537 755	24.0	2%	5%	18%
Guatemala	6 617 244	45.3	3%	13%	30%
Guinea	578 639	5.8	1%	5%	0%
Guinea-Bissau	121 546	7.9	1%	7%	0%
Haiti	3 682 707	38.9	4%	33%	1%
Honduras	2 602 086	32.6	1%	7%	24%
Hungary	5 580 699	58.8	2%	7%	50%
Iceland	15 561	5.3	1%	4%	0%
India	510 352 352	43.8	4%	10%	29%
Indonesia	154 041 488	64.8	13%	22%	29%
Iran	53 001 920	65.7	13%	46%	6%
Iraq	15 049 909	50.3	13%	26%	12%
Ireland	2 874 809	68.3	0%	29%	39%
Israel	7 100 017	96.3	55%	36%	5%
Italy	24 732 976	43.9	4%	10%	30%
Ivory Coast	2 701 444	13.8	7%	7%	0%
Japan	68 692 752	53.6	15%	33%	6%
Jordan	5 896 104	92.0	72%	20%	0%
Kazakhstan	6 660 106	42.2	8%	32%	2%
Kenya	12 296 859	33.3	18%	14%	1%
Korea	23 573 014	47.5	26%	12%	10%
Korea, Dem. People's Rep. of	9 088 182	38.4	15%	14%	9%
Kyrgyz Republic	1 963 812	35.0	6%	24%	4%
Lao People's Democratic Republic	2 490 899	37.8	7%	24%	6%
Latvia	171 627	7.5	1%	4%	2%
Lebanon	3 025 428	75.6	6%	34%	36%
Lesotho	816 929	38.9	10%	29%	0%
Liberia	223 261	4.7	3%	1%	0%
Libyan Arab Jamahiriya	4 566 207	70.2	31%	39%	0%
Lithuania	402 310	11.2	0%	4%	7%
Luxembourg	115 668	23.6	0%	0%	24%
Macedonia	493 688	23.8	0%	11%	13%
Madagascar	6 005 133	28.5	10%	19%	0%
Malawi	5 554 284	39.8	12%	28%	0%
Malaysia	14 221 548	54.1	18%	25%	12%
Mali	2 422 850	15.9	4%	12%	0%
Mauritania	1 258 260	35.5	2%	33%	0%
Mexico	61 046 856	54.1	14%	22%	18%
Mongolia	279 907	9.9	2%	8%	0%
Morocco	24 703 114	69.9	30%	32%	8%
Mozambique	5 025 059	23.1	6%	17%	0%
Myanmar	29 972 088	56.5	21%	26%	10%
Namibia	473 154	23.0	5%	18%	0%
Nepal	11 426 022	39.4	5%	17%	17%

Country/Territory	Population residing in the areas with NDVI decline		Including the share in the areas with,		
	Total	Share of total	NDVI decline detected from the remotely sensed data	NDVI decline likely masked by CO_2 effects	NDVI decline likely masked by chemical fertilization
Netherlands	9 423 244	57.8	4%	18%	36%
New Zealand	2 504 042	62.1	5%	48%	9%
Nicaragua	790 978	12.2	3%	9%	0%
Niger	9 404 559	60.6	6%	54%	0%
Nigeria	9 253 668	6.3	1%	5%	0%
Norway	664 127	14.5	2%	5%	7%
Occupied Palestinian Territory	4 285 492	99.1	71%	27%	1%
Oman	2 649 909	75.3	18%	57%	0%
Pakistan	96 775 024	53.5	8%	21%	25%
Panama	44 240	1.4	0%	1%	0%
Papua New Guinea	1 132 827	19.0	15%	4%	0%
Paraguay	268 279	3.9	1%	3%	0%
Peru	10 228 202	34.3	4%	30%	0%
Philippines	52 496 340	58.4	16%	27%	16%
Poland	14 692 077	38.4	1%	10%	28%
Portugal	1 805 714	17.9	1%	4%	13%
Republic of Moldova	254 014	6.1	0%	2%	4%
Romania	4 467 999	20.5	0%	4%	17%
Russia	15 750 863	11.6	1%	10%	0%
Rwanda	4 825 313	51.2	39%	12%	0%
Saudi Arabia	22 005 500	79.8	4%	70%	7%
Senegal	2 678 271	22.2	1%	21%	0%
Serbia and Montenegro	2 916 383	27.2	1%	4%	23%
Sierra Leone	280 567	4.5	2%	3%	0%
Singapore	4 093 366	91.1	37%	54%	0%
Slovakia	1 507 739	27.8	0%	6%	21%
Slovenia	239 323	10.9	0%	4%	7%
Somalia	5 186 667	39.8	15%	25%	0%
South Africa	16 785 520	37.2	8%	22%	7%
Spain	24 971 382	63.2	9%	21%	33%
Sri Lanka	1 895 356	9.2	1%	1%	7%
Sudan	14 285 319	37.0	9%	28%	0%
Suriname	1 191	0.3	0%	0%	0%
Swaziland	301 288	30.6	7%	24%	0%
Sweden	725 389	8.4	0%	2%	6%
Switzerland	2 317 627	32.9	1%	7%	24%
Syrian Arab Republic	14 839 891	71.5	15%	33%	23%
Taiwan	11 721 754	50.6	12%	21%	18%
Tajikistan	2 789 959	42.2	5%	36%	1%
Thailand	54 005 696	77.6	28%	36%	13%
Togo	1 433 277	24.7	1%	23%	0%
Trinidad and Tobago	482 418	35.5	0%	5%	31%
Tunisia	7 301 244	68.7	13%	32%	23%
Turkey	21 819 756	29.0	3%	8%	17%
Turkmenistan	2 848 499	49.9	1%	49%	0%
Uganda	9 262 307	28.4	12%	17%	0%
Ukraine	5 452 628	12.1	1%	10%	0%
United Kingdom	21 895 624	36.3	1%	6%	29%
United Rep. of Tanzania	19 154 264	43.5	28%	16%	0%
United States of America	92 077 584	29.9	6%	16%	8%
Uruguay	426 312	12.0	2%	9%	1%
Uzbekistan	16 163 704	57.1	2%	24%	31%

Country/Territory	Population residing in the areas with NDVI decline		Including the share in the areas with,		
	Total	Share of total	NDVI decline detected from the remotely sensed data	NDVI decline likely masked by CO_2 effects	NDVI decline likely masked by chemical fertilization
Venezuela	2 255 999	7.9	1%	5%	2%
Viet Nam	53 190 264	60.0	10%	19%	31%
Yemen	16 960 750	62.0	9%	53%	0%
Zambia	4 302 948	33.2	12%	21%	0%
Zimbabwe	7 386 360	49.2	20%	29%	0%
World	**3 215 563 850**	**47%**	**9%**	**19%**	**19%**

Note: This listing of countries and territories does not necessarily reflect the opinion or official position of the authors, their affiliated institutions and of the funding agency on their legal status and are presented here in purely geographic sense.